energy&fuels

Editors' Choice

pubs.acs.org/EF

Review

Review of the Adsorption of Sulfur-Containing Gaseous Pollutants by Biochar: Progress, Challenges, and Perspectives

Published as part of Energy & Fuels special issue "Celebrating Authors of Energy and Fuels Most-Impactful Articles (2022)".

Zihan Xiao, Yangxian Liu,* Jianfeng Pan, and Yan Wang*

Cite This: https://doi.org/10.1021/acs.energyfuels.4c06274

Read Online

ACCESS | Metrics & More | Article Recommendations

ABSTRACT: Sulfur-containing gaseous pollutants (e.g., H_2S, SO_2, and COS) emitted from various industries are important sources of air pollution. Because of the advantages of a simple and clean process, renewability of adsorbent, and cheap raw materials, adsorption removal of sulfur-containing gaseous pollutants by biochar has a good development prospect. However, due to scarce active functional groups and active sites on biochar and an underdeveloped pore structure, the development and application of biochar are still limited in this field. Activation and modification of biochar are one of the most effective ways to raise biochar surface active sites and active functional groups, and improve the pore structure of biochar. This paper reviews the recent research progress of activation and modification methods of biochar for adsorbing sulfur-containing gaseous pollutants (H_2S, SO_2, and COS). Various activation and modification methods are classified and summarized, including acid/alkali activation, microwave activation, metal oxide modification, nitrogen doping modification, and other emerging modification methods. The main process parameters, advantages, and disadvantages of each modification and activation method are introduced in detail. The activation and modification mechanisms as well as the adsorption mechanisms of pollutants are also discussed and summarized. Among these methods, photochemical modification technology has the advantages of a simple and clean process and low energy consumption, and especially it can simultaneously produce oxygen-containing functional groups on the carbon surface and improve the biochar pore structure, showing superior development prospects. This review will provide needed guidance and inspiration for researchers in related areas to develop new biochar-based desulfurization adsorbents.

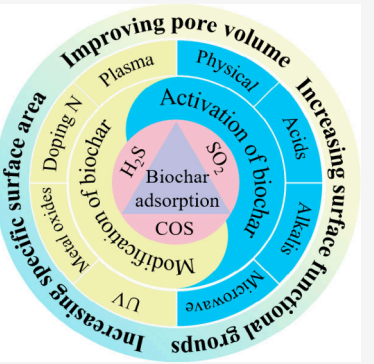

1. INTRODUCTION

Sulfur-containing gaseous pollutants, mainly including hydrogen sulfide (H_2S), sulfur dioxide (SO_2), and carbon oxysulfide (COS), are extremely harmful atmospheric pollutants. H_2S mainly exists in coal/biomass gasification, wastewater treatment, and oil/gas production, which poses a serious threat to human health due to its high toxicity.[1,2] In addition, H_2S will easily corrode equipment (reducing its service life) and poisons the downstream catalysts.[3] H_2S is also easily oxidized to form SO_2, which will become a source of acid rain.[4] SO_2 is mainly produced by volcanic eruptions and the burning of sulfur-containing fuels.[5] The SO_2 discharged into the atmosphere will also form acid rain and smog, which will destroy the ecological environment and damage industrial and civil facilities.[6−8] COS is present in various chemical processes using coal as a feedstock, such as blast furnace gas, yellow phosphorus exhaust gas, and fossil fuel combustion gas, which can corrode equipment and catalysts.[9,10] The presence of COS can also promote the formation of SO_2 by hydrolysis, which thus leads to the production of acid rain and smog, thereby causing air pollution.[11−13] Therefore, the development and research of economically efficient sulfur-containing gaseous pollutant removal technologies is an important topic in this research area.

Most countries in the world have documented laws and regulations to limit sulfur-containing gaseous pollutants emissions. According to the Clean Air Act, the U.S. Environmental Protection Agency (EPA) had a maximum allowable concentration of H_2S of 7 ppm, which is more stringent for special areas such as schools or hospitals. For SO_2, the Clean Air Act specified no more than 500 μg per cubic meter of the atmosphere, while it also lists COS as a hazardous air pollutant. The Economic Commission for Europe had set a Europe-wide emission limit of 10 mg/m^3 for H_2S and 0.2 mg/

Received: December 22, 2024
Revised: January 21, 2025
Accepted: January 24, 2025

Table 1. Pore Parameters and Preparation Conditions of Raw Biochars and Their H_2S and SO_2 Adsorption Capacity and Mechanisms

biochar raw material	pollutant	pyrolysis temperature (°C)	pore parameters SSA[a] (m^2/g)	pore parameters TPV[b] (cm^3/g)	pH	IC[c] (ppm)	AT[d] (°C)	adsorption capacity (mg/g)	main active sites/adsorption mechanism	ref
Camphor	H_2S	400	20.35	/	9.55	50 μL/L	25	109.3	The physisorption is dominant, and the chemical adsorption is promoted by C═O, COO-groups and other functional groups. $HS^- + O \rightarrow S^0 + OH^-$	34
Bamboo			58.01		10.21			336.7		
Rice hull			115.34		10.56			382.7		
Potatoes	H_2S	500	63	/	10	1000	/	53	High pH and C−H, C−O, C═O groups promote H_2S adsorption.	35
Reed	H_2S	500	78	/	9.8	1000	25	60	Containing-oxygen functional groups (−OH, C−O, C═O) promote H_2S oxidation.	36
Lignin	H_2S	450	60	/	10	1000	25	70	Physisorption is dominant. C−O and C−H groups promote chemisorption.	37
Sludge	H_2S	650	48	0.281	9.34	1000	25	20.2	H_2S reacts with metals or metal oxides to produce SO_4^{2-}.	38
Coconut shell	H_2S	/	1030	0.52	6.89	3000	25	112	The physisorption is dominant, and alkaline surface promotes the H_2S dissociation.	39
Sargassum	H_2S	800	26.20	0.034	9.4	200	25	5.8	The physisorption is dominant, and containing-oxygen functional groups, C−O, C═O, COO-, promote H_2S oxidation.	40
Enteromorpha			21.15	0.466	9.1			0.582		
Coffee granules	H_2S	500	/	/	/	970	25	22	$HS^- + O_2 \rightarrow S^0$	41
Almond								230	$HS^- + H_2O + O_2 \rightarrow SO_4^{2-}$	
Perilla	H_2S	700	473.4	0.1	10.6	300	50	18.3	Larger surface area, higher pH, and more containing-nitrogen functional groups promote H_2S removal.	42
Soybean straw		700	420.3	0.2	11.3	300		10.5		
Korean oak	H_2S	400	270.8	0.1	10.2	300	50	6	The adsorption process of H_2S is governed by both physisorption and the local pH within the pores.	
Japanese oak		500	475.6	0.2	9.9	300		5.7		
Cork	H_2S	550	/	/	8.6	750	35	160.44	The physisorption is dominant, and containing-oxygen functional groups (C−O, C═O, COO−) promote the oxidation of H_2S: $H_2S \rightarrow HS^- + H^+$ and $HS^- + O_2 \rightarrow S^0$.	43
		800			9.6			106.32		
Hardwood	H_2S	550	/	/	8.2	750	35	143.47		43
		800			8.7			105.14		
Pig manure	H_2S	500	47.4	/	10.5	1000	20	59.6	C═O and −OH groups, high pH, and metal ions promote	44
Sewage sludge			71.6		8.9			43.97	H_2S to S^0 and SO_4^{2-}	
Cow dung	SO_2	500	4.83	0.014	10.2	5000	25	64.3	Ca^{2+}, K^+, Fe^{3+}, and other metal ions, and high pH together cause SO_2 to produce sulfate.	45
Rice hull			41.5	0.041	9.78			13.3	The excellent pore structure promotes physical adsorption.	
Sludge			10.1	0.022	8.9			34.5	SO_2 reacts with metal ions to form sulfate.	
Palm oil fiber	SO_2	450	1.314	0.0267	6.78	2000	26	18.62	The physisorption is dominant, and C−O, C═O, COOH groups promote the oxidation of SO_2.	27

[a]SSA: Specific surface area. [b]TPV: Total pore volume. [c]IC: Inlet concentration. [d]AT: Adsorption temperature.

https://doi.org/10.1021/acs.energyfuels.4c06274
Energy Fuels XXXX, XXX, XXX−XXX

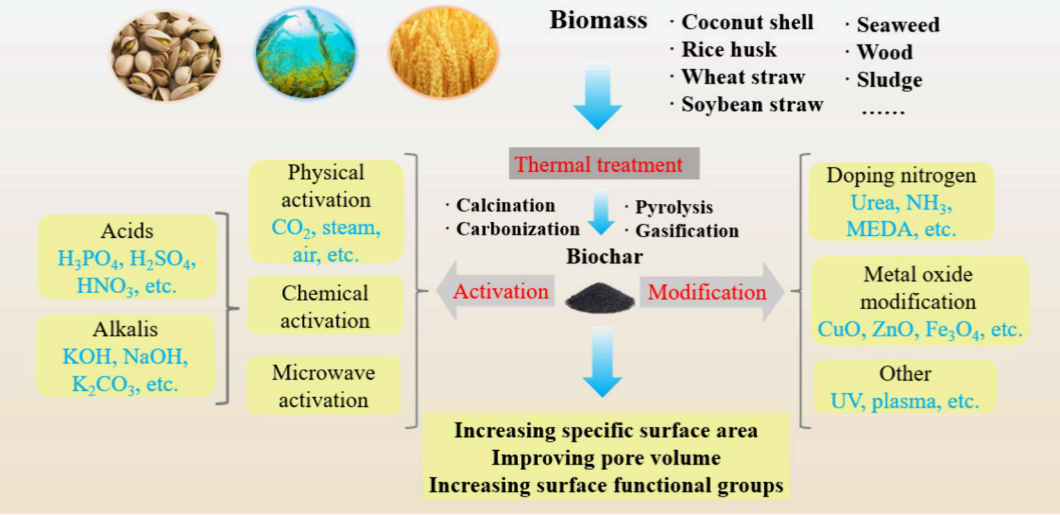

Figure 1. Biochar preparation and activation/modification methods.

m^3 for SO_2 in accordance with the Europe-wide Maximum emission limit for H_2S from combustion installations. In 2018, China had revised the "Natural Gas" to make the requirements for the content of H_2S in natural gas. In this regulation, the content of H_2S in Class I natural gas is less than 6 mg/m^3, and the content of H_2S in Class II natural gas is less than 20 mg/m^3. In 2019, the Ministry of Ecology and Environment of China issued the "Measures to Promote the Implementation of Ultra-Low Emission Standards in Iron and Steel Industry". This regulation stipulates that the SO_2 emission standard for hot blast furnaces, iron-making and heating furnaces, lime kilns, etc. is 50 mg/Nm^3, while the SO_2 emission standard for gas boilers is 35 mg/Nm^3.

At present, common desulfurization technology (i.e., sulfur-containing gaseous pollutant removal technologies) can be roughly divided into wet desulfurization and dry desulfurization. Wet desulfurization technology mainly uses amine solution or alkaline solution to absorb sulfur-containing gaseous pollutants through gas−liquid reactions, which usually can meet the requirements of a high desulfurization load.[9,14] However, there are some problems such as solvent volatilization, high energy consumption, equipment corrosion and scaling, complex product postprocessing and secondary pollution.[15] Therefore, some scholars have begun to pay more attention to dry desulfurization.[16−18] The representative dry removal methods mainly include plasma removal, ozone oxidation, photocatalytic oxidation, photodecomposition, adsorption removal, etc. Among them, the adsorption method has a good prospect because of its advantages such as a simple process, no wastewater generated, and renewable adsorbent. The development of economical and efficient desulfurization adsorbents is the key point in the current research area.

At present, activated carbon (AC), zeolite, metal oxide, metal organic framework compounds (MOFs), biochar, carbon nanotubes, etc. are the common adsorbents in the sulfur-containing gas adsorption field.[19−21] Among them, biochar is an adsorbent with good development prospects due to its wide range of raw materials and low cost. It has been widely shown that biochar can effectively adsorb H_2S, SO_2, NO_X, Hg^0, CO_2, and other gaseous pollutants,[22−27] which possesses good developing prospect and has received increasing attention. Table 1 summarizes the applications of raw biochar in adsorbing sulfur-containing pollutants. However, biochar still has shortcomings such as scarce surface active sites/active functional groups and an underdeveloped pore structure, so it is needed to take various activation and modification methods to enhance the pore structure and surface chemical properties of the biochar, thereby overcoming these challenges.[28] In the past two decades, researchers have proposed and developed many different activation and modification methods for promoting the adsorption performance of biochar for sulfur-containing gaseous pollutants, which mainly include acid/alkali activation, microwave activation, N-doping modification, metal oxide modification, and some other emerging modification methods. Figure 1 shows the common preparation, activation, and modification methods of biochar.

In the past many years, some review articles have introduced the research progress of biochar in adsorption of H_2S, SO_2, and COS. Gwenzi et al.[29] reviewed the development status of air pollutants and greenhouse gases, mainly including SO_2, NO_x, Hg^0, CO_2 and VOCs by biochar. Bamdad et al.[30] reviewed the dynamic and static adsorption isotherms, mechanisms, and process systems of CO_2 and H_2S removal by biochar. Sun et al.[31] reviewed the research advances of the desulfurization process using carbon-based materials, mainly including the introduction of adsorption mechanism and modification methods of H_2S by biomass activated carbon. Wei et al.[32] reviewed the research situation and principle of adsorption of COS from blast furnace gas using porous biochar. Xu et al.[33] reviewed the mechanism and influencing factors of H_2S adsorption by biochar and discussed the methods to enhance the adsorption capacity of H_2S by biochar.

It can be seen that most of the existing reviews mainly focus on the introduction of adsorbent performance and their applications in different fields and mainly use relatively small spaces to introduce the key activation and modification methods of biochar. Besides, most of the existing reviews have been published for over 3−5 years, and some of the results and data in these reviews appear outdated. In recent years, a large number of new research results have been published in the field of sulfur-containing gaseous pollutants by biochar adsorption. It is necessary to publish a new review specifically introducing the recent research advances in activation and modification methods of biochar for adsorbing

https://doi.org/10.1021/acs.energyfuels.4c06274
Energy Fuels XXXX, XXX, XXX−XXX

Table 2. Summary of Pore Parameters, Adsorption Properties, and Mechanism of the Activated Biochar: Acid/Alkali Activation and Microwave Activation

			pore parameters		adsorption performance				
						adsorption capacity (mg/g)			
biochar raw material	pollutant	activation reagents	SSA[a] (m^2/g)	TPV[b] (cm^3/g)	AT[c] (°C)	BD[d]	AD[e]	main active sites/adsorption mechanism	ref
Wood	H_2S	H_3PO_4	1620	1.27	25	/	17.3	High specific surface area and carboxylic acids promote the adsorption of H_2S.	80
Oil palm shell	H_2S	H_2SO_4	1014	/	25	46	76	Phenols and carboxylic acids promote the oxidation of H_2S.	62
		KOH	1148				68	Surface alkalinity is increased, and pyran promotes the decomposition of H_2S.	
Sargassum	H_2S	H_2SO_4	556.56	0.436	25	5.8	8.5	It is mainly physical adsorption, and the pore structure of biochar is improved significantly.	63
Enteromorpha		H2O_2	310.63	0.335		0.58	7.28	Containing-oxygen functional groups such as C−O and COO- promote the oxidation of H_2S.	
Olive pomace	SO_2	H_3PO_4	1456	0.9	30	/	380.17	It is mainly physical adsorption, which is promoted by high specific surface area and big pore volume.	65
Coconut shell	SO_2	HNO_3	971	0.2	100	26	44	C═O and transition state ($\pi-\pi^*$) promote the catalytic oxidation of SO_2 by biochar.	66
Oil palm shell	SO_2	H_3PO_4	1563	/	25	14.55	16.08	It is mainly physical adsorption, and high specific surface area promotes the SO_2 adsorption.	64
		KOH	1408	/			15.34	Pyranone and pyranone promote the adsorption of SO_2	
Walnut shell	H_2S COS	KOH	1239.92	0.766	/	2.5	52.67	Chemisorption and hydroxyl group promotes the oxidation of H_2S.	70
Corncobs	H_2S	KOH	1618	0.8117	25	/	164.54	High specific surface area and good porosity promote the adsorption of H_2S.	81
Chlorella	H_2S	KOH	428.95	0.28	25	Almost	59.1	Containing-oxygen functional groups (−OH, C−O, and C═O) promote the adsorption of H_2S.	74
Spirulina			350.91	0.22		0	42.3		
Sludge and corn stalks	H_2S	KOH	369.27	0.256	50	/	7	The improvement of pore structure and the increase of alkalinity of biochar promote the adsorption of H_2S.	72
Coffee	H_2S	CO_2	2000	/	25	97.3	281.5	Basic functional groups promote H_2S to form S^0.	82
Coconut shell	H_2S	NaOH	815	0.38	25	11.6	105	High pH value and abundant surface metal ions promote the dissociation of H_2S.	83
Coconut shell	H_2S	NaOH	1234	0.44	30	16.7	25	Chemisorption and H_2S reacts with basic compounds to promote the adsorption of H_2S.	84
					550	14	301		
Coconut shell	SO_2	KOH	719	/	230	0.04 mmol/g	0.53 mmol/g	The −OH groups on the biochar surface promote the oxidation of SO_2 to sulfate and SO_3.	77
Waste wood powder	SO_2	KOH	584	0.33	45	60	90	Adsorption capacity of biochar for SO_2 is enhanced by higher specific surface area and better porosity.	78
Silver birch	SO_2	KOH	1700	0.7	25	20.4	35.3	Higher specific surface area promotes the physical adsorption of H_2S.	79
Sewage sludge	H_2S	Microwave	476.87	0.212	35	/	78.4%	Higher specific surface area and more metal irons promote the adsorption of H_2S.	85
Chlorella	H_2S	Microwave	747.2	0.44	25	59.1	96.12	Higher specific surface area and more −OH, C−O, C═O groups promote the adsorption of H_2S.	86
Spirulina		KOH	568.3	0.4		42.3	69.42		
Rice straw	H_2S	Microwave	1999.96	1.191	25	/	57.91	Containing-oxygen functional groups such as C═O, C−O, and COOH promote the oxidation of H_2S to S^0 and sulfate.	87
Wheat straw		KOH	877.16	0.527			61.47		
Sewage sludge	H_2S	Steam Microwave	169.9	0.252	30	/	9.149	Physical adsorption is dominant.	88
		CO_2 Microwave	42.1	0.135			3.415	In the chemisorption, C−O and C═O promote the adsorption of H_2S to produce sulfate and sulfide.	
Coconut shell	H_2S	Microwave	3121	/	/	25.9	77.47	The superior specific surface area and pore structure promote the physical adsorption of H_2S.	89
Conifer sawdust	H_2S	Microwave	367	0.23	25	/	2.6	The presence of mineral substance is favorable for H_2S adsorption.	90
Sludge	H_2S	Microwave H_2O	50.98	/	30	1.47	22.83	Oxygen-containing functional groups and ferric oxide promote the oxidation of H_2S to FeS and SO_4^{2-}.	91
Coconut shell	SO_2	Microwave	646.3	0.344	60	10.9	16.9	Higher specific surface area promotes SO_2 adsorption.	92
								Microwave radiation reduces the acid group, which thus promotes the adsorption of SO_2.	

https://doi.org/10.1021/acs.energyfuels.4c06274
Energy Fuels XXXX, XXX, XXX−XXX

Table 2. continued

biochar raw material	pollutant	activation reagents	pore parameters SSA[a] (m^2/g)	pore parameters TPV[b] (cm^3/g)	adsorption performance AT[c] (°C)	adsorption capacity (mg/g) BD[d]	adsorption capacity (mg/g) AD[e]	main active sites/adsorption mechanism	ref
Coconut shell	SO_2	Microwave	983.7	0.39	60	/	16.36	It is mianly physical adsorption, and the microporous structure promotes the adsorption of SO_2.	93
		Microwave $K_2Cr_2O_7$	866.6	0.28			40.9	Chemisorption, and alcohol and carboxyl groups promote the SO_2 oxidation.	
Oil palm fiber	SO_2	CO_2	270.6	0.16	100	18.62	33	Higher specific surface areas enhance the adsorption capacity of biochar for SO_2.	27
Walnut shell	COS	KOH	484.26	0.272	60	2.5	52.67	Larger specific surface area and pore volume promote the COS adsorption.	70
	H_2S CS_2							The hydroxyl group promotes the oxidation of COS.	
Wood	COS	CO_2	473.61	0.22	/	/	0.234 cm^3/g	It is mainly physical adsorption, and a small part of COS is removed by COS + H_2O → CO_2 + H_2S.	94
								The surface metals facilitate this removal process.	
Coconut shell	COS	KOH	858	0.47	40	5.81	40.64	COS reacts with −OH to form H_2S, which is further oxidized to elemental sulfur and sulfate.	95
Tobacco pole	COS	KOH	1639.8	0.78	60	/	45.25	The excellent pore structure and C−O, -OH functional groups promote the adsorption and hydrolysis of COS.	96
	H_2S CS_2	CO2	699.53	0.32			184.68	The C−O, C═O groups and basic groups promote the hydrolysis of COS and the oxidation of COS to S^0 and sulfate.	

[a]SSA: Specific surface area. [b]TPV: Total pore volume. [c]AT: Adsorption temperature. [d]BD: Before activation. [e]AD: After activation.

sulfur-containing gaseous pollutants (H_2S, SO_2, COS). Therefore, this review discusses the recent research advances of activation and modification methods of biochar for adsorbing sulfur-containing gaseous pollutants (H_2S, SO_2, and COS). Various activation and modification methods are classified and summarized, mainly including acid and alkali activation, microwave activation, metal oxide modification, nitrogen doping modification and other emerging modification methods. The main process parameters, advantages, and disadvantages of each modification and activation method are introduced in detail. The activation and modification mechanisms, as well as the adsorption mechanisms of sulfur-containing gaseous pollutants, have been discussed and summarized. This review will provide needed guidance and inspiration for researchers in the related research areas to develop new biochar-based desulfurization adsorbents.

2. ACID AND ALKALI ACTIVATION

In recent years, carbon-based materials such as activated carbon have been widely used in the adsorption of gaseous pollutants due to their large specific surface area and abundant surface functional groups.[46−48] However, the general commercial activated carbon is made from coal, petroleum, and other fossil fuels, which is expensive, and the source is limited. Compared with activated carbon, biochar is a solid byproduct converted from the pyrolysis of agricultural and forestry waste, etc.[49−51] Due to the wide range of raw material sources and low cost, biochar has become a potential alternative to activated carbon and has received extensive concern in various fields such as water treatment, flue gas purification, and soil remediation.[52−55]

Although biochar has a wide range of sources and low price, its pore structure is underdeveloped, and the active functional groups and active sites on carbon surface are few. Therefore, activation and modification of the biochar are needed through various methods. Activation can generally be divided into physical and chemical activation. The main physical activators are CO_2, O_2, steam, and air or a mixture of them.[56,57] Physical activation is a relatively green way of activation, which can increase the porosity of biochar and also introduce some containing-oxygen functional groups on the surface of biochar.[58] However, the physical activation process requires more energy because the process takes place at high temperatures for a long time.[59,60] Chemical activation mainly uses acids (HNO_3, H_3PO_4, and H_2SO_4) and alkali (KOH, NaOH, and K_2CO_3) to activate biochar. In the process of chemical activation, the pore structure of biochar will be more developed due to the production of gaseous byproducts, and the functional groups introduced on the surface of biochar can also enhance the affinity of biochar for gaseous pollutants. Compared with physical activation, the advantages of chemical activation are that the pore structure is more developed, and the surface sites and active functional groups are also more abundant, which usually has better activation effects.[29,60,61] Table 2 describes the summary of pore parameters, adsorption properties, and mechanisms of the acid/alkali-activated biochars for adsorbing SO_2 and H_2S.

2.1. Acid Activation. *2.1.1. H_2S.* Sulfuric acid is one of the most common acid activators of biochar. Guo et al.[62] used a 40% H_2SO_4 solution to activate oil palm shell biochar at room temperature to remove gaseous H_2S. The results showed that the H_2S adsorption capacity of biochar was 76 mg/g at room temperature, which is better than that of CO_2 and H_2O-activated biochars (46 mg/g and 53 mg/g, respectively). This performance improvement is mainly attributed to the significant increase in oxygen content on the H_2SO_4-activated biochar, which is mainly due to the increase of containing-oxygen functional groups such as carboxyl, phenolic, lactone, and carbonyl groups. The presence of these oxygen-containing functional groups enables the activated oil palm shell biochar surface to undergo chemisorption by forming hydrogen bonds, which can oxidize H_2S into S^0, thus effectively facilitating the removal process of H_2S.

https://doi.org/10.1021/acs.energyfuels.4c06274
Energy Fuels XXXX, XXX, XXX−XXX

In order to further increase the content of containing-oxygen functional groups, Chen et al.[63] used a H_2SO_4/H_2O_2 combination reagent to activate two types of algal biochars (i.e., Sargassum (S) and Enteromorpha morpha (E)) to remove H_2S. Studies have shown that sulfuric acid can improve the pore structure of biochar, while hydrogen peroxide can provide more abundant containing-oxygen functional groups on the biochar surface. Therefore, after the combined activation of these two activators, the specific surface area of biochar is greatly increased by nearly 20 times (S: 26.2 m^2/g to 556.56 m^2/g, E: 21.15 m^2/g to 310.63 m^2/g), and a large number of containing-oxygen functional groups (such as COO−) are produced. Compared with one activator alone, the H_2S adsorption capacity of biochar was better after the combining activation via two activators (S: 5.8 to 8.5 mg/g; E: 0.58 to 7.28 mg/g). It is shown that sulfate is produced after H_2S adsorption on the biochar, which is due to the existence of a large number of containing-oxygen functional groups on the surface of the modified seaweed biochar, so that H_2S molecules are adsorbed on the active sites, and a series of oxidation and/or substitution reactions occur on the modified seaweed biochar surface.

2.1.2. SO_2. Phosphoric and nitric acids are the other two most common acid activation reagents for biochar. Guo et al.[64] activated oil palm shell biochar using H_3PO_4 and KOH with different concentrations, and compared the effects of activator concentration on surface morphology and SO_2 adsorption capacity of biochar. Their study showed that biochar activated with 40% H_3PO_4 had the largest specific surface area (1563 m^2/g) and porosity (72.9%). However, the biochar obtained by the activation of 10% KOH was more conducive to the adsorption of SO_2 (15.34 mg/g). This is because after activation of KOH, some functional groups such as C═O, C═C, C−O, C−H, and so on were produced, which were conducive to the adsorption of SO_2. Yavuz et al.[65] used olive factory waste residue as a raw material and H_3PO_4 as an activator to prepare an olive core biochar for adsorption of SO_2. The results showed that the SO_2 adsorption capacity of biochar was improved after the activation of H_3PO_4, and the SO_2 adsorption capacity of biochar was 380.17 mg/g at 30 °C. The specific surface area significantly increased from 525.2 to 1456 m^2/g and micropore volume increased from 0.22 to 0.59 cm^3/g of biochar with the increase of H_3PO_4 concentration, but the pore size remained unchanged. It is proven that the large specific surface area and pore volume of biochar promote the adsorption of SO_2.

Liu et al.[66] used HNO_3 to activate coconut shell biochar loaded with MnO_2 to study the effect of HNO_3 concentration on the adsorption of SO_2 by biochar. Their results showed that when the adsorption temperature was 100 °C and SO_2 was 500 ppm, the maximum sulfur capacity was 44 mg/g, while the biochar without HNO_3 activation was only 26 mg/g. They found that the specific surface area was decreased from 1012 to 971 m^2/g, and the pore volume was slightly increased from 0.17 to 0.20 cm^3/g after HNO_3 activation. In addition, the number of containing-oxygen functional groups (C−O, C═O) was increased after the HNO_3 activation. When the concentration of HNO_3 was 10 mol/L, the content of the oxygen group C═O was the highest (16.55%). The increase in carbonyl carbon (C═O) and transition ($\pi-\pi^*$) groups on the surface of biochar after the HNO_3 activation effectively promoted the removal of SO_2.

2.2. Alkali Activation. Alkali (KOH, NaOH, K_2CO_3, etc.) is also extensively used to activate biochar because this technology has a simple process and can simultaneously improve the pore structure and surface chemical properties of carbon-based materials.[67−69] The alkali activation can increase the specific surface area, micropore volume basic groups (hydroxyl), and surface alkalinity of biochar, which is conducive to acid gas adsorption. Other studies[70−72] have shown that the alkaline environment is conducive to the formation of elemental sulfur and the improvement of sulfur adsorption capacity.

Activation of biochar by KOH is beneficial to the improvement of its surface morphology, the increase of alkaline groups, and the enhancement of H_2S and SO_2 adsorption capacity. In the process of high temperature activation, CO_2, H_2, and CO are released, which will promote the formation of pores and the improvement of the pore structure. The activation mechanism is described as follows:[73]

$$6KOH + 2C \rightarrow 2K + 3H_2 + 2K_2CO_3 \quad (1)$$

$$K_2CO_3 \rightarrow K_2O + CO_2 \quad (2)$$

$$K_2CO_3 + 2C \rightarrow 2K\ (\text{or}\ K_2O) + 3CO \quad (3)$$

$$K_2O + C \rightarrow 2K + CO \quad (4)$$

$$CO + H_2O \rightarrow CO_2 + H_2 \quad (5)$$

2.2.1. H_2S. Among alkaline activators, KOH is often used as an activator for activating biochar due to its effectiveness and low cost. Li et al.[70] used KOH to activate walnut shell biochar, and studied its ability to simultaneously remove H_2S, COS, and CS_2. Results showed that when the calcination temperature was 600 °C, the KOH/biochar mass ratio was 0.5, and the activation temperature was 700 °C, and the sulfur capacity of the activated walnut shell biochar was 52.67 mg/g. The biochar activated with KOH exhibited the highest specific surface area (increased from 1.28 m^2/g to 1239.92 m^2/g) and pore volume (increased from 0.005 cm^3/g to 0.673 cm^3/g) compared to several other activators (H_3PO_4, $ZnCl_2$, K_2CO_3). In addition, increasing the mass ratio of KOH to biochar resulted in the formation of more micropores and the generation of more alkaline hydroxyl groups, which is favorable for the adsorption of H_2S. XPS analysis showed that most of the products chemisorbed on the biochar surface were elemental sulfur ions (S^0) and sulfate ions (SO_4^{2-}).

Zeng et al.[72] used KOH-activated sludge and corn straw biochar for adsorption of H_2S. Research indicated that when the mass ratio of sludge, corn straw, and potassium hydroxide was 3:7:2, the desulfurization performance was the best, and the H_2S adsorption capacity was 7.00 mg/g, which was 5.74 times that of the unactivated sample. They suggested that KOH activation led to the increase of the specific surface area from 93.215 to 369.27 m^2/g and the increase of the pore volume from 0.14 to 0.256 cm^3/g. While the decrease of lactone groups and the increase of alkaline groups (2.666 mmol/g) created a more alkaline environment, which is conducive for the H_2S removal. During the adsorption, H_2S reacted with the basic functional groups to form elemental sulfur and sulfate.

Ma et al.[74] used KOH solution to activate two kinds of algal biochar (chlorella and spirulina) at room temperature for adsorption of H_2S. Their results showed that the H_2S adsorption capacity of KOH-activated chlorella biochar

https://doi.org/10.1021/acs.energyfuels.4c06274
Energy Fuels XXXX, XXX, XXX−XXX

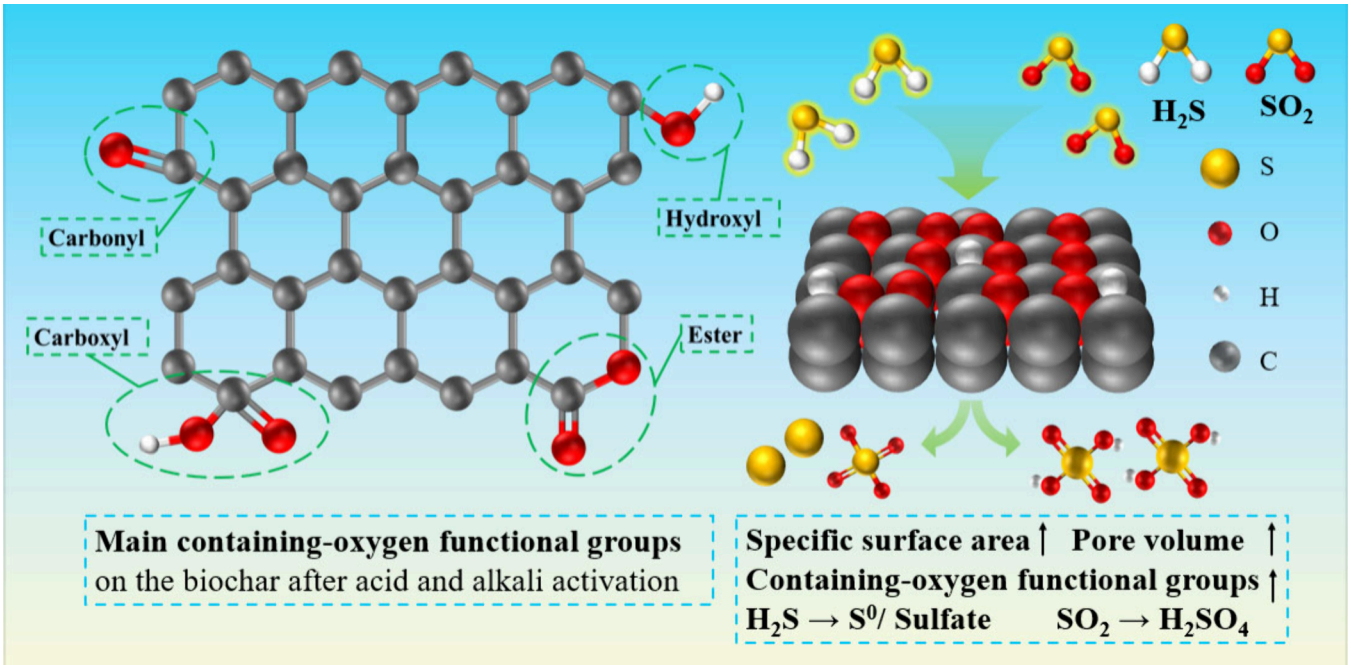

Figure 2. Adsorption mechanisms of H_2S and SO_2 on the biochar after acid/alkali activation.

reached 59.1 mg/g, and that of spirulina biochar was 42.3 mg/g, while the unmodified sample had almost no adsorption capacity under the same studied conditions. After KOH activation, the specific surface area and pore structure of both biochars were significantly improved. The specific surface area of chlorella biochar was increased from 5 to 428.957 m^2/g, while that of spirulina biochar was also increased from 5.653 to 350.91 m^2/g. By measuring the surface pH value of biochar, it was found that the surface pH value was increased from 8.7 to 9.7 after the activation of KOH. In addition, the activation of KOH increased the number of functional groups such as −OH, C═O, and C−O, which promoted the oxidation reaction of H_2S, and the reaction process generated elemental sulfur and sulfate.

In addition to KOH activator, NaOH is also a relatively common alkaline activator due to its cheaper price. Bagreev et al.[75] used NaOH to activate wood biochar to improve its adsorption capacity for H_2S. Results showed that the adsorption breakthrough time of H_2S was increased significantly from 112 to 320 min after NaOH activation. This significant improvement is attributed to the promotion of the H_2S dissociation process by the alkaline environment. Under alkaline conditions, H_2S is more easily dissociated into HS^-, and the addition of sodium hydroxide further increases the pH value of biochar, thus increasing the concentration of HS^-. Subsequently, the HS^- produced is further oxidized and converted into sulfate or carbonate, thus achieving the effective adsorption removal of H_2S on the activated wood biochar.

2.2.2. SO_2. Activation by alkali (KOH, NaOH, etc.) can contribute to the increase of containing-oxygen functional groups on the biochar surface, and the containing-oxygen functional groups are extensively thought to be the key catalytic centers for the oxidation of SO_2 to SO_3.[76] Lee et al.[77] used KOH solution as an activator and prepared a cocoanut biochar for adsorption of SO_2. Results showed that the desulfurization ability of biochar was greatly increased from 0.04 to 0.5298 mmol/g after KOH activation. The characterization results of the biochar surface physical and chemical properties showed that the surface containing-oxygen functional groups (C═O, C−O, −OH) of biochar were greatly increased after KOH activation, and these functional groups played an important role in providing adsorption sites for the selective adsorption of SO_2. They found that in the chemisorption process, the containing-oxygen functional groups could react with SO_2 to form $-SO_4$ groups and $-SO_3$ groups, which greatly promotes the adsorption of SO_2. Due to the action of potassium, the adsorbed SO_2 existed in the form of stable oxide crystals on biochar, such as K_2SO_3 and K_2SO_4. The relevant reactions are as follows:[77]

$$2KOH + SO_2 \rightarrow K_2SO_3 + H_2O \quad (6)$$

$$K_2SO_3 + 1/2O_2 \rightarrow K_2SO_4 \quad (7)$$

$$H_2O + SO_2 + 1/2O_2 \rightarrow H_2SO_4 \quad (8)$$

$$2KOH + H_2SO_4 \rightarrow K_2SO_4 + 2H_2O \quad (9)$$

At high temperatures, due to evaporation of H_2O, the following reaction process can further occur:[77]

$$K_2SO_3 + 2SO_2 \rightarrow K_2SO_4 + 2SO + 1/2O_2 \quad (10)$$

Atanes et al.[78] activated waste wood meal biochar by KOH to remove SO_2 from flue gas. Studies had shown that the SO_2 adsorption capacity of the activated biochar was increased from 20 to 90 mg/g at 45 °C. After KOH activation, the pore structure was optimized, and the specific surface area of biochar was greatly increased from 7 m^2/g to 584 m^2/g. Besides, more containing-oxygen functional groups (such as alcohols, phenols, and carboxyl groups) were introduced onto the activated biochar surface. Their results showed that the adsorption process of SO_2 was mainly physical adsorption. The higher specific surface area and better porosity enhanced the adsorption capacity of biochar for SO_2, and the lower surface acidity was more conducive to the adsorption of SO_2.

https://doi.org/10.1021/acs.energyfuels.4c06274
Energy Fuels XXXX, XXX, XXX−XXX

Table 3. Summary of Pore Parameters, Adsorption Properties, and Mechanisms of the Modified Biochar: Metal Oxide Modification, Nitrogen Doping, and Other Modification Methods

			pore parameters		adsorption performance				
						adsorption capacity (mg/g)			
biochar raw material	pollutant	modification reagents	SSA[a] (m^2/g)	TPV[b] (cm^3/g)	AT[c] (°C)	BD[d]	AD[e]	main active sites/adsorption mechanism	ref
Grapefruit skin	H_2S	$Cu(NO_3)_2{\cdot}3H_2O$	966	0.417	25	12.1	358.3	$CuO + H_2S \rightarrow CuS + H_2O$ $2CuS \rightarrow Cu_2S + S$	116
Rice straw	H_2S	$Cu(NO_3)_2{\cdot}3H_2O$	60.78	0.053	125	/	1191.1	$CuO + H_2S \rightarrow CuS + H_2O$	111
Rice straw	H_2S	$Cu(NO_3)_2{\cdot}3H_2O$	36.05	0.034	120	/	1000.6	$CuO + H_2S \rightarrow CuS + H_2O$ $2CuS \rightarrow Cu_2S + S$	118
Coconut shell	H_2S	$Cu(NO_3)_2{\cdot}3H_2O$	/	/	25	148 min	287 min	$CuO + H_2S \rightarrow CuS + H_2O$	119
Coffee base	H_2S	$CuCl_2{\cdot}2H_2O$	1422	0.655	20	/	132.22	C−O, O−H, C−H groups $Cu_2O + H_2S \rightarrow Cu_2S + H_2O$	117
Peanut shell	H_2S	$CuCl_2{\cdot}2H_2O$	/	/	20	/	97.63	C−O, C−H, C═O groups	67
		$Zn(NO_3)_2$	622.6	0.33			289.3	$ZnO + H_2S \rightarrow ZnS + H_2O$	
Coconut shell	H_2S	$KMnO_4$	191.1	0.15	/	37.7	229	$MnO_2 + 2H_2S \rightarrow MnS_2 + 2H_2O$	123
		$Zn(NO_3)_2 + KMnO_4$	450.3	0.38			334.7	$3Mn_3O_4 + H_2S \rightarrow SO_2 + 9MnO + H_2O$	
Maize straw	H_2S	$FeCl_3{\cdot}H_2O$	34.9	/	/	3.3	8.2	$Fe_3O_4 + 4H_2S \rightarrow 3FeS + 4H_2O + S\ 3S + H_2O + 4O_2 + Fe_3O_4 \rightarrow 3FeSO_4 + H_2O$	124
Maple			59.8	/		6.1	23.9		
Coconut shell	H_2S	$Cu(CH_3COO)_2{\cdot}H_2O\ K_2CO_3$	830	0.49	120	242.1	373.4	The synergistic effect of potassium carbonate and copper oxide promote the production of $\cdot O_2^-$ and then further improve the catalytic activity.	158
Coconut shell	H_2S	$KMnO_4$	390.9	0.131	40	13.8	110.7	$MnO_2 + 2H_2S \rightarrow MnS_2 + 2H_2O$	159
Walnut shell	H_2S	$Mn(NO_3)_2$	921.7	/	350	/	72.4	$3Mn_3O_4 + H_2S \rightarrow SO_2 + 9MnO + H_2O$ $MnO + H_2S \rightarrow MnS + H_2O$	125
Palm kernel shell	H_2S	$MgNO_3{\cdot}7H_2O$	274	0.15	/	30%	98.6%	$MgO + H_2S \rightarrow MgS + H_2O$	160
Palm shell	H_2S	$Ce(NO_3)_3{\cdot}6H_2O$ NaOH	660	0.33	30	1.8	83.1	C═O and COOH groups promote the oxidation of H_2S. $Ce_2O_3 + 3H_2S \rightarrow 2CeS + 3H_2O + S$	126
Wood	H_2S	$Fe(NO_3)_3{\cdot}9H_2O\ Zn(NO_3)_2{\cdot}6H_2O$	1403	0.8	25	5.6	122.5	$ZnFe_2O_4 + 4H_2S \rightarrow ZnS + Fe_2S_3 + 4H_2O$	108
Waste rice	H_2S	$ZnCl_2\ FeCl_3$	1065	0.56	25	12.11	228.29	$ZnFe_2O_4 + 4H_2S + 3/2O_2 \rightarrow$ $ZnS + 2FeOOH + 3H_2O + 3S$	129
Waste rice	H_2S	$Mg(NO_3)_2\ FeCl_3$ Melamine	222.91	0.31	25	15.49	1052.83	$MgFe_2O_4 + 4H_2S + 3/2O_2 \rightarrow$ $MgS + 2FeOOH + 3H_2O + 3S$ Pyridinic-N promotes the dissociation of H_2S.	130
Rice	H_2S	$ZnCl_2\ CaCl_2$	523.6	0.47	25	29.31	834.48	$H_2S + CaCO_3 \rightarrow CaCO_3 + H^+ + HS^-\ ZnO + 4H_2S + 3/2O_2 \rightarrow ZnS + 4H_2O + 3S$	131
Wood	H_2S	$Cu(NO_3)_2Fe(NO_3)_3{\cdot}9H_2O$	1176	0.752	25	214	667	$CuFe_2O_4 + 4H_2S \rightarrow CuS + Fe_2S_3 + 4H_2O$	133
Coconut shell	SO_2	$Cu(NO_3)_2{\cdot}3H_2O$	843	0.416	250	/	43	$SO_2 + 1/2O_2 \rightarrow SO_3SO_3 + CuO \rightarrow CuSO_4$ $CuO + 1/2O_2 + SO_2 \rightarrow CuSO_4$	134
Walnut shell	SO_2	TiO_2	661.8	0.377	90	70	228.62	Metal oxide produces $\cdot O_2^-$ through electron transfer, which promotes the catalytic oxidation of SO_2.	161

https://doi.org/10.1021/acs.energyfuels.4c06274
Energy Fuels XXXX, XXX, XXX−XXX

Table 3. continued

biochar raw material	pollutant	modification reagents	pore parameters SSA[a] (m^2/g)	pore parameters TPV[b] (cm^3/g)	adsorption performance AT[c] (°C)	adsorption capacity (mg/g) BD[d]	adsorption capacity (mg/g) AD[e]	main active sites/adsorption mechanism	ref
		Fe_2O_3	791.0	0.687			125	$TiO_2 + SO_2 \rightarrow TiO + SO_3$	
Palm shell	SO_2	$Ce(NO_3)_3{\cdot}6H_2O$	807	0.33	150	18.62	121.7	$2CeO_2 + SO_2 \rightarrow SO_3 + Ce_2O_3$	162
								Cerium oxide releases the oxygen components through the change of valence state, which thus promotes the oxidation removal of SO_2.	
Straw straw	SO_2	$MgCl_2{\cdot}6H_2O$ Ethylenediamine	138.1	0.36	25	11.1	194.6	N−H groups promote the oxidation removal of SO_2.	113
		Tetraethylenepentamine	139.2	0.42			260	$MgO + 2SO_2 + O_2 \rightarrow SO_3 + MgSO_4$	
Soybean stalks	SO_2	Microwave $Fe(NO_3)_3$	355.6	/	75	96	146	The formed Fe_2O_3 promotes the oxidation of SO_2.	163
								$SO_2 + Fe_2O_3 \rightarrow FeSO_4$	
Coconut shell	H_2S	Urea	808	0.432	30	27.2	54.1	Pyridine-N-oxide and surface chemisorbed oxygen promote the catalytic oxidation of H_2S.	140
		Melamine	732	0.386			71.9		
Palm shell	H_2S	Urea	1000.62	0.51	30	61.1	356.9	Containing-nitrogen functional groups (such as pyridine N, pyrrole N) promote the following reactions: $H_2S \rightarrow H^+ + HS^-$, $HS^- + O \rightarrow S^0 + OH^-$.	144
Sawdust	H_2S	Urea phosphate	1189	0.63	30	0.24	54.8	Pyridine N, pyrrole N and graphitized N increased the adsorption sites, and promotes the following reactions: $H_2S \rightarrow H^+ + HS^-$.	164
Rice hull	H_2S	$NH_3{\cdot}H_2O$	170	0.1	25	2.54	23	Pyridinic-N sites and O* species enhance the conversion of H_2S to S^0.	143
		NH_3	354	0.18			9.58		
Starch	H_2S	$NH_3{\cdot}H_2O$	2084.1	1.004	25	27.13	50.2	Microporous structure and high surface area promote the physical adsorption of H_2S.	145
		Alanine	1613	0.796			110.7	Pyridinic-N sites and quinonyl promote the dissociation of H_2S to HS^-.	
Poplar sawdust	H_2S	Melamine cyanuric acid ester	1914.3	0.82	30	1.0	1827	Ultra high N content (17.2 atom %) and microporous channel structure promote the adsorption of H_2S.	149
Cypress wood	H_2S	Melamine	1839.0	1.12	25	12.5	426.2	Pyridinic/pyrrolic nitrogen atoms promote the adsorption of H_2S.	148
Cypress sawdust waste	H_2S	Melamine cyanurate (MCA)	805	0.5	25	48.76	390.1	Containing-nitrogen functional groups such as pyridinic and pyrrolic promote the conversion of H_2S to HS^-.	165
Sludge Pine sawdust	H_2S	Urea	1065	0.78	25	72.9	356.5	The high nitrogen content and pyridine nitrogen promote the conversion of hydrogen sulfide to S^0 and sulfate.	150
Soybean straws	SO_2	NH_3	371.1	/	30	92.8	175.9	Pyridines, pyrroles and microporous structure promote the adsorption of SO_2.	155
					120		115.4		
Sludge poplar bark	SO_2	$NH_3{\cdot}H_2O$	108	0.09	70	46.3%	55.9%	H_2O, pyridine-N and pyrrole-N promote the adsorption of SO_2.	157
Corncobs	SO_2	Diethanolamine (MDEA) -methanol	654.0	0.32	120	58.0	216.9	The adsorption site is the N-Q group, which is converted to N oxide after the SO_2 adsorption, and SO_2 is converted to SO_4^{2-}.	156
Corncobs	SO_2	MDEA	Near0	Near 0	120	57.8	156.2	Quaternary N, C−N, and N−H groups promote SO_2 to produce sulfate.	166
Soybean straws	SO_2	NH_3+CO_2	500.2	/	30	98.6	201.9	Hydrogen bond of dimeric, π-type, polymeric, chelation and bridge promote SO_2 to form sulfate.	142
					120	58.6	143.68		

Table 3. continued

biochar raw material	pollutant	modification reagents	pore parameters		adsorption performance			main active sites/adsorption mechanism	ref
			SSA[a] (m^2/g)	TPV[b] (cm^3/g)	AT[c] (°C)	adsorption capacity (mg/g) BD[d]	adsorption capacity (mg/g) AD[e]		
Walnut shell	H_2S	NH_3-plasma	640.9	0.2954	60	/	390 min	The pore structure is improved, and the functional groups such as C═O/O−O−O, O−C═O, amino groups promote the oxidation of H_2S to S^0 and SO_4^{2-}.	167
Corn stalks	H_2S	UV H_2O_2	535.44	0.31	25	2 min	24 min 90.9	UV/H_2O_2 modification increases the surface containing-oxygen groups, such as -OH, C−O, COO- groups, which promotes the removal of H_2S.	168
Soybean straws	SO_2	UV CO_2	347.28	0.37	70	/	100.181	CO_2 activation promotes the formation of micropores. UV modification promotes the formation of containing-oxygen functional groups (carboxyl).	169
Tobacco stem	COS	$Cu(NO_3)_2Fe(NO_3)_3$	554	0.29	60	/	231.28	Metal oxides facilitate the hydrolysis of COS and promotes the following process: $COS + CuO + H_2O \rightarrow CuO{\cdot}H_2S + CO_2$	170
Coconut shell	COS	$Cu(NO_3)_2$	768.4	0.3	20	7.5	14.8	Containing-oxygen functional groups (such as hydroxyl, carboxyl, etc.) and metal oxides participate in the adsorption of COS, and the adsorption product is sulfate.	171
Tobacco pole	H_2S COS CS_2	$Cu(NO_3)_2$	514.77	0.26	60	/	161.93	Metal oxides and −OH groups promote the hydrolysis of COS, and the H_2S produced by hydrolysis is oxidized to elemental sulfur and sulfate.	96

[a]SSA: Specific surface area. [b]TPV: Total pore volume. [c]AT: Adsorption temperature. [d]BD: Before modification. [e]AD: After modification.

https://doi.org/10.1021/acs.energyfuels.4c06274
Energy Fuels XXXX, XXX, XXX−XXX

Braghiroli et al.[79] compared the SO_2 adsorption capacity of birch biochar activated by CO_2, steam and KOH, respectively. Research indicated that the biochar activated by KOH had the largest specific surface area and porosity (1700 m^2/g and 0.7 cm^3/g), and the SO_2 adsorption capacity was increased from 20 to 35.3 mg/g. Functional groups such as phenols, lactones, and carboxyl groups were abundant on the surface of biochar activated by KOH. In contrast, the steam-activated biochar had a relatively lower specific surface area (590 m^2/g), but possessed a higher SO_2 adsorption capacity (76.9 mg/g). This is because the steam-activated biochar has fewer acidic groups and therefore resulted in a higher SO_2 adsorption capacity. Figure 2 shows the types of the main oxygen-containing functional groups on the surface of biochar after the acid/alkali activation and the adsorption mechanisms of H_2S and SO_2.

3. METAL OXIDES MODIFICATION

Metals oxides (e.g., Fe, Mn, V, Ti, Ce, Cu, Co, Ni, etc.) are often used as desulfurization adsorbents due to their strong affinity with sulfur-containing gases.[97−102] However, pure metals and metal oxides used as adsorbents usually suffered from evaporation, sintering, and mechanical disintegration, which will result in the loss of specific surface area and porosity, thereby adversely affecting their performance and lifetime.[103] To overcome these problems and improve the removal performance, the metals can be loaded onto the support materials with a high specific surface area.[103−107] The large surface area and high porosity of the support materials can contribute to the high dispersion of metal oxides, and the pore channels of the support materials can limit the growth of metal oxide particles.[108−110] Related research[41,60,111−114] had shown that the combination of metals and biochar materials could effectively increase the surface active sites of biochar, enhance the electron transfer on carbon surface, and improve the reactivity between biochar and gas pollutant molecules, thereby strengthening the adsorption capacity of adsorbent for H_2S and SO_2. Table 3 shows the summary of pore parameters, adsorption properties, and adsorption mechanisms of the metal oxide-loaded biochar for adsorption of H_2S and SO_2. Figure 3

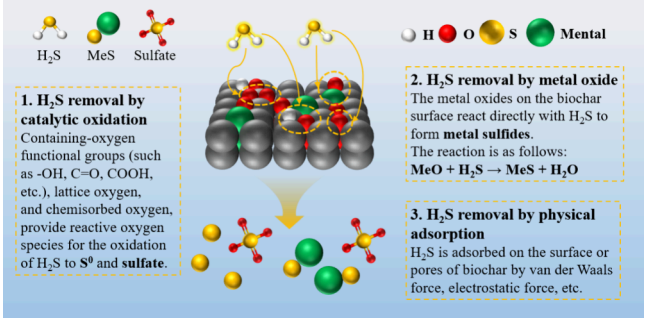

Figure 3. Mechanism of H_2S adsorption by metal oxide-supported biochar.

and Figure 4 show the adsorption processes of H_2S and SO_2 on biochar loaded with metal oxides, respectively. The corresponding chemical reactions are as follows:[115]

$$H_2S + MeO \rightarrow MeS + H_2O \quad (11)$$

$$MeO_2 + SO_2 \rightarrow MeO + SO_3 \quad (12)$$

3.1. H_2S. *3.1.1. Single Metal Modification.* Copper-based oxides are one of the most common biochar modification reagents for enhancing the H_2S removal because of its high sulfur balance constant, high desulfurization accuracy, and good dispersion.[111,116−119] Cui et al.[111] used microwave-activated rice straw biochar as the carrier, and prepared a CuO-loaded rice straw biochar (CuWRS) to study its adsorption capacity of H_2S. Studies showed that the breakthrough time of H_2S increased from 11 to 78 min after loading CuO. When the calcination temperature was 300 °C and the Cu/WRS mass ratio was 2.56, the adsorption effect was the best, and the sulfur capacity could reach up to 1191.1 mg/g, which is more than many similar Cu-based adsorbents. It was found that although copper loading reduced the specific surface area of biochar (280 m^2/g to 60.78 m^2/g), a large number of CuO adsorption active sites with strong oxidation ability were formed on biochar, which greatly enhanced H_2S removal. In the adsorption process, lattice oxygen participated in the chemisorption, and Cu^{2+} in CuO was reduced. The main products were CuS and small amounts of $CuSO_4$ and Cu_2S.

Zhao et al.[118] used a waste Cu-based Fenton-like reagent as a modifier reagent to prepare CuO-loaded straw biochar to remove H_2S. Results showed that the maximum H_2S adsorption capacity of the modified biochar was 1000.6 mg/g at a calcination temperature of 300 °C and reaction temperature of 120 °C. The modification of the waste Cu-based Fenton-like reagent greatly promoted the increase of biochar surface metal active sites, but led to the decrease of the specific surface area and the pore volume of the adsorbent from 280.07 m^2/g to 36.06 m^2/g, and from 0.1 cm^3/g to 0.034 cm^3/g, respectively. CuO was found to be the key active substance to promote the chemisorption of H_2S on the adsorbent. The main products of the reaction between H_2S and CuO on the adsorbent were determined to be copper sulfide, cuprous sulfide, and elemental sulfur. The reaction processes between copper based-modified biochar and H_2S can be described by the following chemical reactions:[117,118]

$$CuO + H_2S \rightarrow CuS + H_2O \quad (13)$$

$$Cu_2O + H_2S \rightarrow Cu_2S + H_2O \quad (14)$$

$$Cu_2S + 2Cu_2O \rightarrow 6Cu + SO_2 \quad (15)$$

Zinc-based oxides have good potential to adsorb H_2S at room temperature due to good thermodynamics at room temperature, which have been widely studied as a desulfurization agent.[120,121] Hernandez et al.[122] prepared plant biochar loaded with ZnO by a precipitation method, and then studied the adsorption capacity of H_2S at room temperature. Studies had shown that the loading of metal oxides provided more active sites for H_2S removal, which made the H_2S adsorption capacity of biochar significantly increase, and the H_2S adsorption capacity was 11.8 times that of the original biochar. After modification, there were well dispersed ZnO particles on the surface of biochar. The specific surface area was increased from 851 to 867 m^2/g, and the pore volume was increased from 0.44 to 0.45 cm^3/g. The reaction process between H_2S and ZnO on the active sites can be depicted as follows:

$$ZnO + H_2S \rightarrow ZnS + H_2O \quad (16)$$

Zhang et al.[123] used $Zn(NO_3)_2$ solution to impregnate coconut shell biochar and prepared the coconut shell biochar modified by ZnO to adsorb H_2S. Results showed that the pore

https://doi.org/10.1021/acs.energyfuels.4c06274
Energy Fuels XXXX, XXX, XXX−XXX

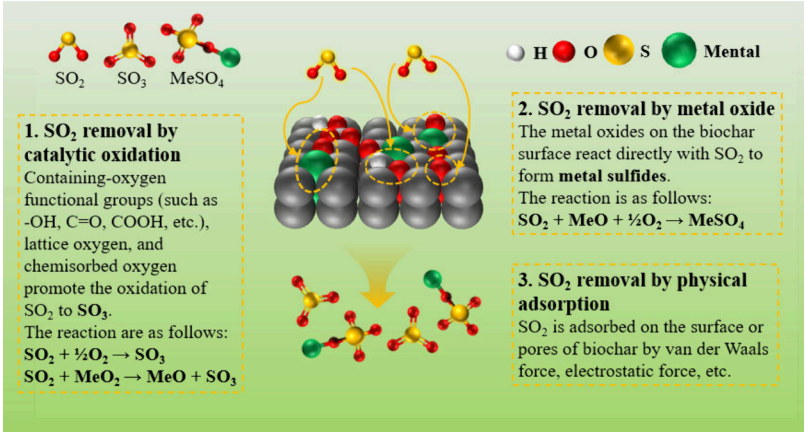

Figure 4. Mechanism of SO_2 adsorption by metal oxide-supported biochar.

plugging (0.36 cm^3/g to 0.33 cm^3/g) caused by ZnO loading reduced the specific surface area (from 685.7 m^2/g to 622.6 m^2/g). However, the increase of active sites on biochar greatly increased the H_2S adsorption capacity of biochar (from 37.7 to 289.3 mg/g), and the adsorption effect was better than that of MnO_2-loaded biochar (229 mg/g). On the biochar, H_2S was chemically adsorbed with ZnO and other active sites, and the catalytic oxidation process of H_2S was promoted by the functional groups (C−O, COO-, and -OH) on the biochar surface.

In addition to copper-based oxides and zinc-based oxides, other metal oxides such as iron-based oxides and manganese-based oxides are also used to modify the biochar to improve the adsorption performance of H_2S. Choudhury et al.[112,124] used as a modifier to load Fe_3O_4 on corn stover (CSB) and maple (MB) biochar to remove H_2S from biogas. Results indicated that the H_2S adsorption capacity of Fe_3O_4-loaded biochar was increased 2.5−3.9 times. The H_2S adsorption capacity of CSB was increased from 3.3 to 8.2 mg/g, and the H_2S adsorption capacity of MB was increased from 6.1 to 23.9 mg/g. A large amount of ferric oxide on the surface of biochar provided the active sites for the chemisorption of H_2S, and during the H_2S adsorption process, reactive oxygen species and metal oxides on the biochar facilitated the conversion of sulfides to elemental sulfur and sulfate.

Wang et al.[125] impregnated walnut shell biochar with supercritical water and $Mn(NO_3)_2$ solution, and prepared biochar loaded with Mn_xO_y of different valence states to adsorb H_2S. Results showed that when the activation temperature was 350 °C, the biochar had the highest specific surface area (921.7 m^2/g), and the H_2S adsorption capacity increased from 42.9 mg/g to 72.4 mg/g. They found that different carriers and different impregnation temperatures had different effects on the valence state of Mn, and the catalytic oxidation activity of Mn_xO_y to H_2S varied with different valence states. XRD results showed that when the impregnation temperature was 350 °C, the active sites on the surface of biochar mainly existed in the form of Mn_3O_4 and a small amount of MnO, and the reactions between these sites and H_2S can be expressed as follows:[125]

$$3Mn_3O_4 + H_2S \rightarrow SO_2 + 9MnO + H_2O \quad (17)$$

$$MnO + H_2S \rightarrow MnS + H_2O \quad (18)$$

Lau et al.[126] used NaOH and $Ce(NO_3)_3{\cdot}6H_2O$ to impregnate palm shell biochar and prepared an alkali-activated biochar loaded with CeO_2 to remove H_2S. Results demonstrated that when the Ce content was 5%, the H_2S adsorption capacity of biochar was 83.1 mg/g. They found that Ce_xO_y could provide an oxygen component for the oxidation of H_2S through the conversion between CeO_2 and Ce_2O_3. NaOH could improve the surface alkalinity of biochar and increase the contents of C−O, C═O, and COOH and other functional groups, thereby enhancing the adsorption of H_2S on the surface of biochar. During the adsorption process, Ce^{4+} was reduced, and S^{2-} was oxidized into S^0, sulfite, and sulfate (S^0 was the main product).

3.1.2. Multimetallic Modification. In addition to the use of single metal for modifying biochar, the use of multimetals for modifying biochar has also been widely studied due to the synergistic catalytic effects generated between different metals.[123,127−129] Yuan et al.[129] used rice as raw material and $ZnCl_2$ and $FeCl_3$ as activators, and then prepared a waste rice biochar modified by $ZnFe_2O_4$ to achieve the adsorption of H_2S. Results showed that the sulfur capacity of the biochar prepared at 500 °C was greatly increased from 12.1 mg/g to 228.29 mg/g. Compared with the specific surface area of the original biochar of 2.76 m^2/g, the modified biochar had a high surface area of 1065 m^2/g. It was found that there were hydroxyl groups and nitrogen−oxygen functional groups on the surface of the modified biochar, which contributed to the adsorption and dissociation of H_2S. Besides, the activators $ZnCl_2$ and $FeCl_3$ had better pore formation effects for biochar, and the $ZnFe_2O_4$ was well dispersed on the biochar, without obvious metal oxide agglomeration. The $ZnFe_2O_4$ loaded on the surface of biochar provided abundant active sites for the H_2S adsorption, which played an important role in the removal of H_2S. The reaction mechanism is as follows:[108]

$$H_2S \rightarrow HS^- + H^+ \quad (19)$$

$$HS^- + O_2 \rightarrow S + H_2O \quad (20)$$

$$ZnFe_2O_4 + 4H_2S + 3/2O_2 \rightarrow ZnS + 2FeOOH + 3H_2O + 3S \quad (21)$$

Yuan et al.[130] used melamine as the nitrogen source, and $Mg(NO_3)_2$ and $FeCl_3$ as metal activators to prepare a nitrogen-doped waste rice biochar loaded with $MgFe_2O_4$ for adsorption of H_2S. Results showed that the sulfur capacity of biochar was greatly increased from 15.49 mg/g to 1052.83 mg/g. After $MgFe_2O_4$ modification, the desulfurization process was a

https://doi.org/10.1021/acs.energyfuels.4c06274
Energy Fuels XXXX, XXX, XXX−XXX

combination of catalytic oxidation and reactive adsorption, in which the presence of pyridine-N and C−O, O−C═O and other containing-oxygen functional groups on the biochar surface greatly enhanced the dissociation and oxidation of H_2S, while the $MgFe_2O_4$ promoted the direct reactive adsorption of H_2S. The reaction mechanism is as follows:[130]

$$MgFe_2O_4 + 4H_2S + 3/2O_2 \rightarrow MgS + 2FeOOH + 3H_2O + 3S \quad (22)$$

Yuan et al.[131] prepared a $CaCO_3$−ZnO loaded rice biochar using $ZnCl_2$ and $CaCl_2$ solution as the mixed modifier to remove H_2S. Research indicated that the prepared biochar after modification had a high sulfur capacity. At 25 °C, the sulfur capacity was increased from 29.31 to 834.48 mg/g, and the specific surface area was increased from 102 to 523 m^2/g after modification. They found that there was a certain amount of nitrogen in the modified biochar, mainly existing in the form of pyridine and pyrrole. The containing-nitrogen groups produced effectively contributed to the formation of alkaline water films to promote the catalytic oxidation of H_2S. The adsorption process of H_2S on the modified biochar was mainly summarized as follows: (i) H_2S is oxidized into S^0 after dissociation, and part of S^0 is oxidized into H_2SO_4, which then further reacts with $CaCO_3$ to produce $CaSO_4$; (ii) H_2S directly reacts with ZnO to produce ZnS. The reaction mechanism is as follows:[131]

$$H_2S \xrightarrow{CaCO_3} HS^- + H^+ \quad (23)$$

$$2HS^- + O_2{}^* \rightarrow 2S + 2OH^- \quad (24)$$

$$ZnO + 4H_2S + 3/2O_2 \rightarrow ZnS + 4H_2O + 3S \quad (25)$$

$$H_2O + S + 3/2O_2 \rightarrow H_2SO_4 \quad (26)$$

$$H_2SO_4 + CaCO_3 \rightarrow CaSO_4 + H_2O + CO_2 \quad (27)$$

Yang et al.[108] studied the ability of $ZnFe_2O_4$ loaded biochar to remove H_2S at room temperature. Research showed that when the $ZnFe_2O_4$ loading was 10 wt%, the H_2S adsorption capacity of the adsorbent was the largest, reaching a maximum value of 122.5 mg/g, but the H_2S adsorption capacity of the unmodified wood activated carbon was only 5.6 mg/g. They found that $ZnFe_2O_4$ was highly dispersed on the biochar matrix and provided a large number of active sites for the H_2S adsorption. The reaction process between $ZnFe_2O_4$ and H_2S is as follows:[132]

$$ZnFe_2O_4 + 4H_2S \rightarrow ZnS + Fe_2S_3 + 4H_2O \quad (28)$$

Moreover, due to the instability of the generated Fe_2S_3, the following reactions will occur, which further greatly improves the removal ability of H_2S:[132]

$$Fe_2S_3 \rightarrow FeS + FeS_2 \quad (29)$$

$$FeS + FeS_2 + 3/2O_2 + H_2O \rightarrow 2FeOOH + 3S \quad (30)$$

$$2FeOOH + 3H_2S \rightarrow Fe_2S_3 + 4H_2O \quad (31)$$

Chen et al.[133] used $Cu(NO_3)_2$ and $Fe(NO_3)_3{\cdot}9H_2O$ as activators to synthesize the wood biochar loaded with $CuFe_2O_4$ to adsorb H_2S. Results showed that the H_2S adsorption capacity of the biochar was increased from 214 mg/g to 667 mg/g at room temperature when the metal load was 20 wt%. The removal process of H_2S included two pathways: active adsorption and catalytic oxidation. In the desulfurization process, the formed FeOOH acted as a catalyst intermediate, which promoted the production of products (including sulfides, elemental sulfur, and sulfates). Micropores could enhance the dispersion of catalysts, provide the adsorption centers, and store the products. The S^0, as the main product, was mainly produced in the micropores.

3.2. SO_2. Loading metal oxides on biochar can also improve the adsorption capacity of SO_2 through an increase in surface adsorption sites and catalytic centers. Tseng et al.[134] used $Cu(NO_3)_2{\cdot}3H_2O$ solution to prepare a coconut shell biochar loaded with CuO to adsorb SO_2. Results showed that when the copper load was 3 wt%, the SO_2 adsorption capacity of biochar was 25 mg/g. In the adsorption process, when O_2 was present, SO_2 was catalyzed on the copper phase to produce SO_3, and then it reacted with CuO to produce $CuSO_4$. In addition, SO_2 could also react directly with CuO to produce $CuSO_4$. The reaction mechanism is as follows:[134]

$$SO_2 + 1/2O_2 \rightarrow SO_3 \quad (32)$$

$$SO_3 + CuO \rightarrow CuSO_4 \quad (33)$$

$$CuO + 1/2O_2 + SO_2 \rightarrow CuSO_4 \quad (34)$$

Fan et al.[135] loaded Fe_2O_3, MnO_2 and pyrolusite onto the walnut shell biochar, respectively, and prepared Fe_2O_3, MnO_2, and Fe_2O_3-MnO_2 loaded biochars to adsorb SO_2. Results showed that the sulfur capacity of the biochar loaded by metal oxides was significantly increased compared to that of the original biochar (123.8 mg/g). When the adsorption temperature was 80 °C, the SO_2 adsorption capacities of the three biochars were 140.6 mg/g, 157.8 mg/g, and 227.8 mg/g, respectively. They observed that Fe_2O_3 loaded biochar had a larger specific surface area and pore volume (515.5 m^2/g to 641.1 m^2/g, 0.37 cm^3/g to 0.43 cm^3/g), while MnO_2 loaded biochar was more conducive to the formation of functional groups (such as C−OH, C−O, C═O); thus the MnO_2 loaded biochar had a stronger catalytic effect on SO_2. Compared with single metal oxide loading, Mn and Fe in pyrolusite were more dispersed, and the pore structure development of biochar was more favorable (687 m^2/g and 0.45 cm^3/g) due to the synergistic effect of the metal mixture in pyrolusite, which resulted in higher catalytic activity for SO_2. In the adsorption process, SO_2 was first oxidized into SO_3, and then it was further converted into H_2SO_4. The related reactions are as follows:[135]

$$Fe_2O_3 + SO_2 \rightarrow SO_3 + FeO \quad (35)$$

$$2MnO_2 + SO_2 \rightarrow 2SO_3 + Mn_2O_3 \quad (36)$$

$$SO_3 + H_2O \rightarrow H_2SO_4 \quad (37)$$

Chen et al.[113] used $MgCl_2{\cdot}6H_2O$ as a modifying agent to prepare straw biochar loaded with MgO by a coprecipitation method to remove SO_2. Research indicated that, compared with the sulfur capacity of the original biochar (11.1 mg/g), the SO_2 adsorption capacity of the MgO-loaded biochar was up to 194.6 mg/g. It was found that after modification by $MgCl_2{\cdot}6H_2O$, the high sulfur capacity of the biochar was attributed to the increases of active sites (abundant Mg−O active sites were formed), and larger specific surface area and pore volume (from 10.6 m^2/g to 138.1 m^2/g and 0.03 cm^3/g to 0.4 cm^3/g, respectively). Sumathi et al.[136] compared the SO_2 adsorption capacities of palm shell biochar loaded with

https://doi.org/10.1021/acs.energyfuels.4c06274
Energy Fuels XXXX, XXX, XXX−XXX

different metal oxides (NiO, Fe_2O_3, CeO_2, V_2O_5). Results showed that the specific surface area and pore volume of biochar were all reduced after the modification of different metal oxides, but the SO_2 adsorption capacities were all increased. The adsorption capacity of SO_2 is based on the following order: CeO_2 > V_2O_5 > NiO > Fe_2O_3. The high SO_2 adsorption capacity of palm shell biochar loaded with CeO_2 was attributed to the stronger oxidation ability and higher oxygen storage of CeO_2.

4. DOPING NITROGEN MODIFICATION

Nitrogen doping modification for biochar has attracted extensive attention because of the several advantages such as rich containing-nitrogen functional groups and developed porous structure.[22,137,138] The doped nitrogen atoms can replace the adjacent carbon atoms in porous carbon to improve the electronegativity, which can raise the electron transfer in carbon skeleton and enhance the electrostatic dipole−dipole effect, thereby resulting in better adsorption and catalytic activity.[22,139,140] Besides, nitrogen doping modification can also improve the alkalinity and hydrophobic degree of the biochar surface,[137,139,141,142] thereby resulting in better adsorption effects for SO_2 and H_2S. Common nitrogen doping reagents mainly include urea, ammonia, melamine, and so on. The common nitrogen doping methods mainly include endogenous nitrogen doping and exogenous nitrogen doping. Related studies[143−145] had showed that using different nitrogen sources, doping methods, and process parameters to modify biochar would lead to different pore structures, nitrogen contents, and containing-nitrogen functional group types on the carbon surface, which will result in different adsorption performances of biochar for sulfur-containing gaseous pollutants. This section mainly introduces the recent research progress on the adsorption of sulfur-containing gaseous pollutants by nitrogen-doped biochar. Figure 5 shows the

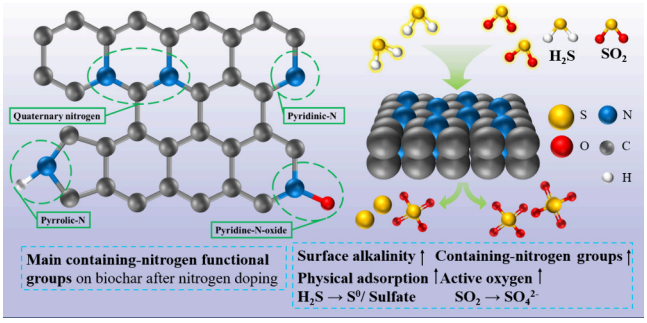

Figure 5. Adsorption mechanism of H_2S and SO_2 on N-doped biochar.

adsorption mechanisms of H_2S and SO_2 by biochar after nitrogen loading. Table 3 shows a summary of pore parameters, adsorption properties, and mechanisms of the nitrogen-doped biochar for adsorption of H_2S and SO_2.

4.1. H_2S. Nitrogen-doped biochar has been shown to be an efficient metal-free catalyst for H_2S removal at room temperature.[146,147] Nor et al.[144] used urea to modify palm shell biochar with a microwave-assisted activation to remove H_2S. Results showed that the H_2S adsorption capacity of the modified biochar was greatly increased from 61.14 mg/g to 356.94 mg/g, which were mainly attributed to the following aspects: (i) the specific surface area of the modified biochar was increased, and some new pores were formed in the existing pores; (ii) new containing-nitrogen functional groups were produced on the biochar, which effectively increased the surface alkalinity and Lewis basic sites of the biochar.[148] Hu et al.[145] used $NH_3{\cdot}H_2O$ and alanine as nitrogen sources to prepare nitrogen-doped starch porous biochar by a hydrothermal carbonization method and then used it to study the adsorption capacity of H_2S. Results indicated that the H_2S adsorption capacity of the alanine-modified biochar was 110.7 mg/g, which was better than that of the $NH_3{\cdot}H_2O$-modified biochar (50.2 mg/g), while the original biochar was only 27.13 mg/g. They discovered that $NH_3{\cdot}H_2O$ could promote the formation of micropores and mesoporous pores, expand the storage space of reaction products, and increase the specific surface area and pore volume of biochar (1491.5 m^2/g to 2084.1 m^2/g, and 0.72 cm^3/g to 1.0 cm^3/g). However, alanine was more conducive to the formation of containing-nitrogen functional groups, forming pyridine-N and quinone groups on the biochar, which had strong adsorption, dissolution, and oxidation capacity for H_2S. In the desulfurization process, pyridine-N and quinone groups promoted the removal of H_2S. The main product of the desulfurization process was S^0, and the byproducts were sulfuric acid and sulfonic acid. After nitrogen doping, the contents of S^0 and sulfuric acid were increased by 5.65 and 1.73 times, respectively.

Setiawan et al.[143] used biogas fermented digestion solution as a sustainable ammonia source to prepare a nitrogen-doped biochar (N2) and compared the H_2S removal ability of the biochar modified with pure NH_3 (N1). Results showed that the adsorption of H_2S on the biochar was significantly improved after doping with nitrogen. The adsorption capacities of N1 and N2 for H_2S were 9.58 and 23.0 mg/g, respectively, while the H_2S adsorption capacity of the original biochar was only 2.54 mg/g. They indicated that the surface of N1 had more containing-nitrogen functional groups, including pyridine-N, pyrrole-N, and graphite-N, among which pyridine-N dominated. The presence of pyridine-N promoted the formation of the O* species on the biochar, which effectively enhanced the redox reaction, thus promoting the chemical adsorption of H_2S. The improvement of N_2 adsorption capacity was due to the higher utilization rate of micropores so that the diffusion of H_2S in micropores was not hindered by the formation of sulfate. Wu et al.[149] prepared nitrogen-doped poplar sawdust biochar (NBAC) with a high nitrogen content and microchannel structure for H_2S adsorption using melamine cyanuric acid (MCA) as a nitrogen source. Results showed that the adsorption capacity of NBAC for H_2S reached 1827 mg/g, while the biochar without MCA was only 1 mg/g. They found that the prepared biochar had a microchannel structure with layered pores, which was conducive to mass transfer and storage of elemental sulfur, and H_2S could continue to be catalyzed and oxidized on NBAC after multiple layers of sulfur covered the nitrogen sites. They indicated that during the H_2S adsorption process, the ultrahigh nitrogen content (17.2 atom %) on the surface of biochar provided a large number of active sites (such as pyridine N, pyrrole N, etc.) for the catalytic oxidation of H_2S and the formation of sulfur radicals. These active sites effectively enhanced the dissociation of H_2S on the carbon surface, which enabled the rapid oxidation of HS^- into S^0, thus promoting the removal of H_2S.

Through using urea as a nitrogen source, and sludge and pine sawdust as raw materials, Li et al.[150] prepared a nitrogen-

https://doi.org/10.1021/acs.energyfuels.4c06274
Energy Fuels XXXX, XXX, XXX−XXX

doped biochar for adsorption of H_2S. Their results showed that the H_2S adsorption capacity of biochar was significantly increased from 72.9 mg/g to 365.5 mg/g after urea modification. The specific surface area of biochar was increased from 155 to 1065 m^2/g, and the pore volume was increased from 0.07 to 0.78 cm^3/g. Moreover, the modified biochar surface is rich in nitrogen-containing functional groups such as pyrrole nitrogen and pyridine nitrogen, which enhanced the conductivity and molecular polarity of biochar and promoted the adsorption of H_2S. It was found that during the adsorption, H_2S was mainly oxidized into S^0 and sulfate.

4.2. SO_2. As a Lewis acid, SO_2 tends to interact with basic surfaces; that is, the sulfur atom in SO_2 as the electron acceptor can effectively form stable complexes with the bases as the electron donor.[151] Relevant studies[60,152,153] had shown that the alkaline groups on the surface of biochar, such as alkenes, quinones, benzene, etc., were the groups with high affinity for SO_2, which was conducive to the adsorption of SO_2. To investigate the effects of containing-nitrogen functional groups on the adsorption of SO_2, Qu et al.[154] investigated the possible interaction between SO_2 and N species on carbon surface by DFT. Their results showed that nitrogen doping could improve the physical adsorption of SO_2 on carbon surface by increasing the van der Waals force between carbon surface and SO_2 molecule, and the presence of various containing-nitrogen functional groups effectively contributed to electrostatic interactions for adsorption of SO_2 (such as hydrogen bonding and dipole interactions).

Zhang et al.[142] explored the SO_2 adsorption properties of soybean straw biochar modified by high temperature treatment of CO_2-NH_3. Results showed that after the modification, the specific surface area of biochar was greatly increased from 0.04 m^2/g to 500.21 m^2/g, and the micropore volume was also significantly increased from 0.1 cm^3/g to 0.22 cm^3/g. Besides, the contents of the containing-nitrogen groups such as pyridine-*n*-oxide, quaternary N, and pyridine on the biochar surface were clearly increased. Due to the significant improvement in the physicochemical properties of biochar, when the adsorption temperature was 120 °C, the sulfur capacity was increased from 57 to 145.68 mg/g. It was found that trimers and bridging hydrogen bonds were the main adsorption sites for SO_2 adsorption. With the increase of adsorption temperature, the containing-nitrogen groups as the main adsorption sites could combine with SO_2 to form sulfamide (60 °C), which eventually existed in a more stable form of SO_4^{2-} (120 °C). Zhang et al.[155] used NH_3 to modify soybean straw biochar to remove SO_2. Results showed that the SO_2 adsorption capacity of the NH_3-modified biochar was increased from 100 to 175.9 mg/g at 30 °C and that the sulfur capacity was positively correlated with the nitrogen content of biochar. They indicated that during the modification process, due to the decomposition of NH_3 into H, N, NH, amino, and other free radicals, thermal corrosion occurred on the surface of biochar, which formed new narrow micropores (specific surface area and pore volume increased from 0.04 to 371.11 m^2/g and 0.1 to 0.2 cm^3/g, respectively) and introduced containing-nitrogen functional groups on the surface of biochar. The adsorption process was mainly a physical adsorption, and after NH_3 modification, a large number of pyridine and pyrrole appeared on the surface of biochar to promote the removal of SO_2.

Zhang et al.[156] used methyl diethanolamine (MDEA)-methanol solution to prepare nitrogen-doped corncob biochar for SO_2 removal, and they studied the effect of NO on SO_2 removal. Results showed that the nitrogen content of biochar was greatly increased from 0.44% to 9.5% after MDEA impregnation. At 120 °C, the sulfur content of the corn cob biochar was increased from 58 to 216.9 mg/g. They found that at a low concentration of NO, NO and SO_2 combined to form $NO_2 \cdot SO_3$ intermediates, which promoted the adsorption of SO_2. However, at high concentrations of NO, NO, and SO_2 competed for the same adsorption sites, thereby hindering the adsorption of SO_2. The main adsorption sites on the biochar were found to be the N-Q group of quaternary nitrogen, which was transformed to N oxide after the adsorption of SO_2, while SO_2 was converted to SO_4^{2-} in the presence of H_2O and oxygen. Wang et al.[157] modified sewage sludge biochar with ammonia−water to adsorb SO_2. Results showed that after ammonia−water modification, the surface containing-nitrogen functional groups of the biochar was increased significantly (0.11% to 3.57%). The doping of nitrogen atoms changed the uniform electrostatic potential distribution and the surface polarity of the biochar. H_2O, pyridine functional groups, and pyrrole functional groups could promote the adsorption of SO_2 on biochar. Pyridine enabled the formation of dipole−dipole interactions and hydrogen bonds between SO_2 and H_2O, while pyrrole enabled the formation of hydrogen bonds between SO_2 and H_2O.

Nitrogen-doped biochar can effectively improve the adsorption of SO_2 by biochar. It is found that the containing-nitrogen functional groups can not only improve the physical adsorption capacity of biochar for SO_2 but also promote the chemical adsorption of biochar for SO_2. Among them, the enhancement of SO_2 physical adsorption caused by nitrogen incorporation is always related to the increase of basicity, the change of local electron density, the polarity of carbon atoms, and the charge distribution on the carbon surface. At the same time, the excess π-electrons in the containing-oxygen functional group can be transferred to adsorbed oxygen to form superoxide ions, which can oxidize SO_2 into SO_3 and then further produce sulfuric acid.[142,152,157] In general, nitrogen modification and doping are beneficial for the development of pores, the enhancement of electronic transfer capability, and the increase of the specific surface area and pore volume of the biochar. Besides, through increasing containing-nitrogen functional groups, the surface alkalinity of biochar is also improved, which is conducive to the adsorption and oxidation of SO_2 ($SO_2 \rightarrow SO_4^{2-}$). Figure 5 shows the adsorption mechanism of H_2S and SO_2 by biochar after nitrogen modification and doping.

5. MICROWAVE ACTIVATION

Traditional heating can not provide a uniform temperature for samples of different shapes and sizes, and the temperature gradient in the sample will lead to high energy consumption and a long heating time.[172] As a kind of electromagnetic energy, the microwave can overcome the disadvantage of traditional heating from outside to inside, which can achieve uniform and rapid heating of objects without a temperature gradient.[173−175] Microwave radiation may produce materials with new microstructure and induce some unique chemical reactions that can not be induced by conventional heating.[176] In addition, microwave heating also has the advantages of a shorter heating time, lower energy consumption, selective heating, greener process, etc. Based on the above several advantages, microwave heating has attracted more and more

https://doi.org/10.1021/acs.energyfuels.4c06274
Energy Fuels XXXX, XXX, XXX−XXX

attention in the field of materials synthesis and catalysis field.[173−175] Related studies[85,90,93,174−176] have shown that the use of microwave heating to activate biochar can effectively improve the pore structure of biochar and introduce some new functional groups onto biochar, thus strengthening the adsorption of gaseous pollutants. This section introduces the adsorption performance and mechanisms of sulfur-containing gas pollutants by microwave-activated biochar.

5.1. H_2S. Lin et al.[85] activated sludge biochar for 10 min at 650 °C by microwave heating and studied the adsorption capacity of the microwave-activated biochar for H_2S. Their results showed that the desulfurization efficiency of the activated biochar was 78.4%. The microwave-activated biochar had a more developed pore structure and higher surface alkalinity, which promoted the adsorption of H_2S. Besides, due to the presence of metal elements on the surface of sludge biochar, these metal species could catalyze H_2S to form metal sulfide and sulfate, thereby increasing the H_2S adsorption capacity of biochar. Cui et al.[87] studied the effect of microwave-assisted KOH activation on H_2S removal by rice straw biochar (WKRS) and wheat straw biochar (WKWS). Results showed that the sulfur capacity of the microwave-assisted KOH activated biochar was significantly higher than that of original biochar, which was 57.911 and 61.446 mg/g, respectively. The pH value of biochar was increased (WKRS: 9.5 to 9.6; WKWS: 9.9 to 10.3), and the pore structure of biochar was also greatly improved (WKRS: 108 to 1991.96 m^2/g, 0.186 to 1.191 cm^3/g; WKWS: 154.92 to 877.15 m^2/g, 0.217 to 0.527 cm^3/g). In addition, the numbers of containing-oxygen functional groups (such as C═O, C−OH, and/or C−O) on the biochar surface were significantly increased, which were involved in the chemisorption process of H_2S, and both S^0 and sulfate were produced on the biochar surface.

Dou et al.[86] activated chlorella (CKW) and spirulina (SKW) biochar with microwave-assisted KOH for H_2S adsorption. Results showed that compared with thermal KOH activated biochar, the H_2S adsorption capacity of the two biochars after microwave-assisted KOH activation was enhanced (CKW: 59.1 to 96.12 mg/g; SKW: 42.3 to 69.42 mg/g), and the specific surface area and pore volume of the two biochars significantly increased (CKW: 5 m^2/g to 747.22 m^2/g, 0.01 cm^3/g to 0.44 cm^3/g; SKW: 5.65 m^2/g to 568.3 m^2/g, 0.1 cm^3/g to 0.4 cm^3/g). Moreover, the contents of surface functional groups (−NH and C−O) were significantly increased, and the contents of C═O and C−H were also slightly increased. They found that the H_2S adsorption process was mainly physical adsorption supplemented by chemical adsorption. When chemical adsorption occurred on the carbon surface, -NH and C−O were involved in the adsorption process of H_2S, and the products were S^0 and sulfate. Xu et al.[88] activated the sludge biochar by microwave pyrolysis and CO_2/steam activation, and then studied the H_2S adsorption capacity of the activated biochar. Results showed that the sulfur capacity of the steam-activated sample was higher than that of the CO_2-activated sample, which was 9.149 and 3.451 mg/g, respectively. The specific surface area of the original biochar was only 34.2 m^2/g, which was increased to 169 m^2/g after microwave steam activation and 42.1 m^2/g after microwave CO_2 activation, respectively. They found that there were acidic functional groups (methylene) on the surface of the unactivated samples that were eliminated after microwave activation. The contents of C═O, C−O, and other groups were increased after microwave activation, which promoted the adsorption of H_2S. In the adsorption process of H_2S, physical adsorption was dominant, while chemical adsorption produced sulfate, sulfone, and sulfide.

Zhu et al.[91] prepared a kind of sludge biochar by a microwave-assisted steam activation method, and then modified it using red mud. They further studied the adsorption capacity of the prepared biochar for H_2S. The results showed that the specific surface area of the biochar after microwave steam activation was 50.98 m^2/g compared with 28.5 m^2/g of the original biochar, and the H_2S adsorption capacity of biochar was significantly increased from 1.47 to 22.83 mg/g. They found that the number of oxygen-containing functional groups (such as C−O, C═O, and O−C ═O, etc.) on the activated biochar surface was increased, which facilitated the adsorption and catalytic oxidation of H_2S. In addition, the iron oxide on the biochar surface reacted with H_2S to form FeS, which was subsequently further oxidized to produce SO_4^{2-}.

5.2. SO_2. Zhang et al.[92] activated the coir organisms biochar by microwave heating for adsorption of SO_2. Results showed that the SO_2 adsorption capacity of biochar was increased from 10.9 to 16.9 mg/g after microwave activation. They found that after microwave activation, the acidic functional groups on the surface of biochar were gradually decreased from 0.238 to 0.063 mmol/g, and the surface alkalicity of biochar was increased owing to the generation of alkaline functional groups on the surface of biochar, which effectively promoted the adsorption of SO_2 through acid−base interaction. In addition, alkaline functional groups had high electronic conductivity, which thus further enhanced the adsorption of SO_2 on the biochar surface.

Fengrui et al.[93] used microwave-assisted oxidant ($K_2Cr_2O_7$) to activate coir biochar, and then studied the ability of the activated biochar to adsorb SO_2. Research indicated that compared with the biochar activated by microwave-oxidizer ($K_2Cr_2O_7$−CAC), the biochar activated by direct microwave (CAC) had larger specific surface area and pore volume (983.7 m^2/g > 866.6 m^2/g, 0.39 cm^3/g > 0.28 cm^3/g), and a large number of microporous scale structures were found on the surface of biochar. The optimal SO_2 adsorption capacity of $K_2Cr_2O_7$−CAC was 40.09 mg/g, which was 2.45 times that of CAC. They indicated that the adsorption process of SO_2 was mainly chemical adsorption, and $K_2Cr_2O_7$ introduced a large number of alcohol and carboxyl groups to the surface of biochar, which greatly promoted the adsorption of SO_2. Table 2 describes the summary of pore parameters, adsorption properties, and mechanisms of the microwave-activated biochars for adsorbing SO_2 and H_2S.

6. MODIFICATION BY OTHER METHODS

In recent years, nonthermal plasma has been widely applied for material surface modification due to its simple process, high modification efficiency, and low secondary pollution.[23,177,178] Ning et al.[167] used nonthermal plasma to modify walnut shell biochar loaded with Fe_2O_3 for adsorption of H_2S. Research demonstrated that nonthermal plasma treatment significantly improved the H_2S adsorption capacity of biochar. When the treatment time was 10 min and the output voltage was 6.8 kV, the sample maintained 100% H_2S removal efficiency within 390 min, which was much higher than 120 min of the original biochar. The reasons for this enhancement effect are summarized as follows: (i) the specific surface area, pore volume, and micropores of biochar are all increased after nonthermal plasma modification, which is beneficial for the physical adsorption and molecular transfer of H_2S; (ii) the contents of containing-oxygen and containing-nitrogen functional groups such as C═O/O−C−O,

https://doi.org/10.1021/acs.energyfuels.4c06274
Energy Fuels XXXX, XXX, XXX−XXX

O−C═O, amino groups, etc. on the biochar are all increased after the nonthermal plasma modification, thus enhancing the adsorption of H_2S; (iii) the conversion of chemisorbed oxygen into lattice oxygen after the nonthermal plasma modification effectively promotes the catalytic oxidation removal of H_2S.

Hydroxyl radical (·OH) is recognized as a type of clean and efficient strong oxidant, which has been widely applied in many fields such as wastewater treatment, soil remediation, flue gas treatment and so on.[179−183] Zhao et al.[168] used UV/H_2O_2 advanced oxidation process to produce ·OH, and then used it as a modifier to modify the corn straw biochar to remove H_2S. Results showed that after the modification by UV/H_2O_2 advanced oxidation process, the desulfurization breakthrough time of the modified corn stalk biochar was greatly increased from 2 to 24 min (reaching 90 mg/g), and its H_2S adsorption capacity was better than that of commercial activated carbon and most biochar adsorbents. It was found that the modification by UV/H_2O_2 advanced oxidation process effectively improved the pore structure of biochar, and significantly increased the numbers of containing-oxygen functional groups (−OH, C−O, COO−) on the surface of biochar, thus greatly promoting the removal of H_2S on the biochar. Elemental sulfur and sulfate are found to be the main adsorption products.

Chen et al.[169] prepared a modified soybean straw biochar using CO_2 as an activator and UV radiation modification for adsorption of SO_2. Results showed that when the UV radiation modification temperature was 100 °C and the modification time was 12 h, the sulfur capacity of the modified biochar was 100.181 mg/g, which was 3.41 times that of the original biochar. They found that UV radiation modification effectively promoted the formation of micropores in the biochar. The specific surface area was increased from 114.22 m^2/g to 347.28 m^2/g, and the pore volume was increased from 0.12 cm^3/g to 0.37 cm^3/g. After the UV radiation modification, some lactones and hydroxyl groups on the surface of biochar were oxidized to the carboxyl group. The content of carboxyl group on the surface of biochar was increased from 0.473 mmol/g to 0.539 mmol/g, and the surface alkalinity and nitrogenous basic functional groups (such as pyridine-N and pyrrole-N) were also both increased, which enhanced the adsorption and oxidation capacity of the sample for SO_2. Table 3 describes the summary of pore parameters, adsorption properties, and mechanisms of the biochars modified by other methods for adsorption of SO_2 and H_2S.

7. COS ADSORPTION BY BIOCHAR

At present, catalytic hydrolysis, as the mainstream COS removal technology, has the advantages of mild reaction, high conversion rate and mature technology.[184] However, the catalytic hydrolysis process will lead to a large amount of sulfur or sulfate deposition on the catalyst surface, resulting in the blockage of pores and the poisoning and deactivation of the catalyst. Besides, the reaction process is long and is easy to corrode the equipment.[32,185,186] Recently, the adsorption removal technology of COS by biochar has received gradually increasing attention due to its simple and cleaning process. Sakanishi et al.[94] studied the adsorption and decomposition of H_2S and COS by wood biochar in the temperature range of 300 to 450 °C. Study showed that although the specific surface area of biochar was smaller than the commercial activated carbon (473.61 m^2/g > 1059.77 m^2/g), the adsorption capacity was higher (0.234 cm^3/g > 0.039 cm^3/g). This was because the residual metal in biochar could effectively promote the removal of COS, and the COS will form H_2S and CO_2 in the pores. Compared with the chemisorption of H_2S on biochar, the adsorption of COS on biochar was mainly controlled by physical adsorption, most of COS was adsorbed by biochar in the pores, and only a small part of COS was decomposed into CO_2. Sattler et al.[187] compared the adsorption capacity of three carbon-based materials for COS, in which the biochar prepared by coconut husk and coal was named VPR. They studied the effects of H_2O and H_2S on COS adsorption. Research indicated that the sulfur capacity of VPR was 1.8 mg/g at a 17% relative humidity. With the increase of H_2S concentration and relative humidity, the adsorption capacity of COS by the biochar was decreased because H_2O/H_2S and COS could compete the adsorption sites on the carbon surface.

The comparative study of different activators has a certain reference value for the rational selection of activators. Li et al.[70] activated walnut shell biochar with different activators (H_3PO_4, KOH, $ZnCl_2$, K_2CO_3) for simultaneous removal of H_2S, COS, and CS_2 from yellow phosphorus tail gas and closed calcium carbide furnace tail gas. Results showed that KOH-activated biochar had the best desulfurization effect. When the mass ratio of KOH to biochar was 0.5, the sulfur capacity of biochar was increased from 2.5 to 52.67 mg/g. This was because KOH could react with carbon materials to form a large number of micropores at high temperature, which greatly raised the specific surface area and pore volume of biochar (from 1.28 m^2/g to 484.26 m^2/g and 0.005 cm^3/g to 0.272 cm^3/g, respectively). Moreover, KOH activation provided a large number of hydroxyl functional groups and increased the alkaline adsorption sites on the biochar. The adsorption products were mainly S^0 and SO_4^{2-}. It was also found that increasing the activation temperature and the amount of KOH increased the specific surface area (1239.92 m^2/g) but also led to the transformation from micropores to mesoporous pores, thereby resulting in a decrease in COS adsorption capacity (52.67 to 45.25 mg/g). The micropores with 0.3−1.8 nm was found to play an important role in the COS adsorption process.

In addition to terrestrial biochar, the adsorption performance of seaweed biochar for COS was also been tested. Hanaoka et al.[188] prepared a kind of seaweed biochar for COS adsorption by gasification under 900 °C and CO_2/O_2 atmosphere. Their results showed that the prepared seaweed biochar had a specific surface area of 71 m^2/g and a pore volume of 16.3 cm^3/g. At 450 °C, the biochar had a good simultaneous removal capacity of H_2S and COS, and nearly 99.5% of the COS was removed by the seaweed biochar. This was because the chemisorbed H_2S promoted the decomposition of COS. At the same time, the metal oxides on the surface of biochar could promote the chemisorption of COS, and COS could react with the metal oxides in biochar to form the (Ca and Mg) crystalline phase. The reaction processes are as follows:[188]

$$CaCO_3{\cdot}MgO + COS \rightarrow CaS{\cdot}MgO + 2CO_2 \quad (38)$$

$$CaO{\cdot}MgO + COS \rightarrow CaS{\cdot}MgO + CO_2 \quad (39)$$

Sun et al.[170] prepared tobacco biochar loaded with CuO and Fe_2O_3 by a solution−gel method to simultaneously remove H_2S, COS, and CS_2. Research showed that when the temperature was 60 °C, the humidity was 49%, the oxygen content was 0.5%, and the sulfur capacity reached 231.28 mg/g. It was found that low humidity was conducive to the adsorption of COS on biochar, while high humidity would form a water film on the surface of the biochar to hinder the diffusion of COS in the pores. In the adsorption process, the existence of appropriate oxygen and C═O, -OH groups on the surface of biochar could enhance the hydrolysis and oxidation process of COS, and metal oxides loaded on the biochar were also conducive to active adsorption of COS (COS + CuO +

https://doi.org/10.1021/acs.energyfuels.4c06274
Energy Fuels XXXX, XXX, XXX−XXX

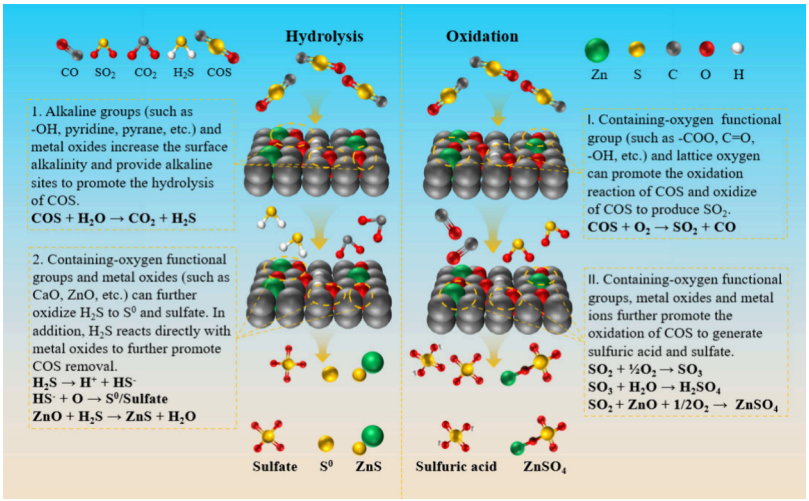

Figure 6. Chemical mechanism of COS removal on biochar.

$H_2O \rightarrow CuO{\cdot}H_2S + CO_2$). The main adsorption products were the thiol/thioether, S^0, and sulfate.

Wang et al.[95] used KOH impregnation to activate coconut shell biochar to study the adsorption capacity of the modified biochar for COS. Their results showed that when the KOH mass fraction was 10%, the COS adsorption capacity of biochar was increased from 5.81 mg/g to 40.64 mg/g. This is due to the increase of the −OH functional group on the surface of biochar after KOH impregnation, which increases the surface alkalinity of biochar and promotes the hydrolysis and catalytic oxidation process of COS. In the adsorption process, COS can react with the −OH functional group to form H_2S (the produced H_2S can be further oxidized into elemental sulfur and sulfate), and it can also be directly oxidized into sulfate. Li et al.[171] used an equal-volume impregnation method to prepare two kinds of modified biochars from coconut shell biochar through using $AgNO_3$ and $Cu(NO_3)_2$ as two types of modification reagents, and then further studied their COS adsorption capacities on the prepared two kinds of modified biochars (i.e., Ag/AC and Cu/AC). Their results showed that the maximum COS adsorption capacity of Cu/AC was 14.8 mg/g when the Cu load was 5%, which was better than that of Ag/AC (nearly 10.0 mg/g) and raw biochar (7.5 mg/g). It was found that after modification, the surface of biochar was loaded with metals and metal oxides, among which the surface of biochar after $AgNO_3$ treatment was loaded with Ag, while the surface of biochar after $Cu(NO_3)_2$ treatment was loaded with Cu_2O. Therefore, Cu/AC achieved a stronger COS adsorption activity than Ag/AC. The containing-oxygen functional groups (such as hydroxyl, carboxyl, etc.) and metal oxides all participated in the adsorption process of COS, and the adsorption product was mianly sulfate.

Different modification methods usually have different effects on the physical and chemical properties of biochar,[96] Ruan et al.[96] compared the effects of chemical activation and physical activation on the simultaneous removal of H_2S, COS, and CS_2 on tobacco stem biochar. They used KOH, H_3PO_4, $ZnCl_2$, and K_2CO_3 to chemically activate the biochar, respectively. Results showed that the adsorption capacity of the biochar activated by KOH was the highest (45.25 mg/g), while the adsorption capacities of the biochar activated by the other three activators were 10.03 12.09, and 20.35 mg/g, respectively. This was because the specific surface area and pore volume of the biochar after activation by KOH were both the largest, reaching 1639.8 m^2/g and 0.78 cm^3/g, respectively. The excellent pore structure effectively promoted COS removal. After the KOH activation, the numbers of C−O, −OH, and other functional groups on the biochar surface were increased, which was conducive to the simultaneous removal of H_2S, COS, and CS_2. In addition, they used H_2O and CO_2 to physically activate the biochar, respectively. Results showed that the adsorption capacity of the biochar activated by CO_2 was 184.68 mg/g, which was far higher than that of the biochar activated by H_2O (98.32 mg/g). Compared with the H_2O-activated biochar, the CO_2-activated biochar had a larger specific surface area, more C−O, C═O groups, and alkaline groups, thus promoting the hydrolysis of COS. During the adsorption process, in addition to the physical adsorption of COS, COS was also hydrolyzed to produce H_2S, and then H_2S was further oxidized into S^0 and sulfate. Ruan et al.[96] studied the simultaneous removal of H_2S, COS, and CS_2 by tobacco stalk biochar modified with different metal nitrates ($Fe(NO_3)_3$, $Cu(NO_3)_2$, $Co(NO_3)_2$, $Ni(NO_3)_2$, $Zn(NO_3)_2$). Research showed that the adsorption capacity of the biochar modified by $Cu(NO_3)_2$ was the strongest, and the adsorption capacity reached 161.93 mg/g when the CuO load was 10%. Then, based on the biochar loaded with CuO, the authors further studied the adsorption capacity of the biochar loaded with two types of metal oxides. Their results showed that the desulfurization capacity of the biochar modified with Cu and Fe was the strongest, up to 231.28 mg/g. They found that the metal oxides promoted the hydrolysis and catalytic oxidation of COS. During the adsorption process, CuO was reduced into Cu_2O, and then COS was finally oxidized into S^0 and metal sulfate. Table 2 and Table 3 further describe the summary of pore parameters, adsorption properties, and mechanisms of the biochars for adsorption of COS.

Based on the above review and analysis, it can be found that the removal mechanism of COS on biochar mainly involves hydrolysis and catalytic oxidation.[95,186,189] In the hydrolysis process, alkaline groups (such as −OH, pyridine, pyranes, etc.) and metal oxides increase the surface alkalinity and promote the hydrolysis of COS to produce H_2S and CO_2.[32,185,190] The generated H_2S is further oxidized into elemental sulfur and sulfate by catalytic oxidation of containing-oxygen functional groups and lattice oxygen on biochar.[96,170] In addition, H_2S

https://doi.org/10.1021/acs.energyfuels.4c06274
Energy Fuels XXXX, XXX, XXX−XXX

can react with metal oxides to form metal sulfide.[188,189] In the catalytic oxidation process, various containing-oxygen functional groups (such as −OH, C−O, C═O, etc.), lattice oxygen, and chemisorbed oxygen can promote the oxidation reactions of COS to produce SO_2 and CO.[95,96,191] After this, the resulting SO_2 can be further oxidized into sulfuric acid and sulfate.[95,96,171] The above mechanism of COS can also be more intuitively described in Figure 6.

8. CHALLENGES AND PERSPECTIVES

Based on the above analysis and comments, the main challenges and perspectives of this review are summarized as follows:

(1) Acid and alkali activation can simultaneously improve the pore structure and increase the surface active sites of biochar, making it one of the most widely used methods for biochar activation. However, high temperature and high energy consumption, reagent leakage, and strong corrosion are unavoidable challenges for this technology. Thus, the development of the new modification methods that possess milder operating conditions, lower energy consumption, and a cleaner process is the key direction of development in this field. Advanced oxidation technologies have received more and more attention because they can generate hydroxyl radicals, sulfate radicals, and superoxide radicals with extremely strong oxidizing properties. These free radicals are environmentally friendly and may be applied for modifying biochar to raise the functional groups and active sites and improve the pore structure of biochar. This is likely to become a promising development direction because a large number of advanced oxidation processes have been developed in the fields of water treatment and flue gas treatment. Microwave activation have received increasing attention due to their uniform and rapid heating method, as well as the ability to generate unique physical and chemical changes on the surface and inside of biochar. However, microwave activation can lead to the removal of active functional groups and active sites on the surface of biochar due to extreme conditions. Therefore, after microwave activation, the combined use of other chemical modification methods, especially clean advanced oxidation processes, may be a worthwhile approach to explore.

(2) Transition metal oxides (e.g., Cu, Zn, Mn, Fe, Ce, etc.) have been proven to be a promising class of sulfur-containing gaseous adsorption and catalytic materials owing to good affinity for sulfur. Single metal modification leads to limited improvement in adsorption capacity, while the combined modification of multiple metals often can produce modification effects beyond expectations due to the synergistic effect between multiple metals. However, current research in this field is still insufficient, especially in the synergistic modification between transition metal oxides and various rare earth elements (utilizing their superior oxygen storage capacity of rare-earth metal oxides), which deserves more research. Besides, excessive metal loading onto biochar can lead to deterioration of the pore structure of adsorbent and a decrease in its activity, as well as waste of metal active components. Single atom catalysts have gained great attention in the field of catalysis and adsorption due to their relatively low cost, high catalytic activity, and good selectivity, which can realize high catalytic activity, and simultaneously alleviate deterioration of adsorbent and reduce reagent consumption. Therefore, the development of various single metal and multimetal single atom catalysts and the hybrids with biochar is worth exploring.

(3) Doping nitrogen into biochar can raise the adsorption capacities of H_2S and SO_2 and improve the adsorption selectivity of biochar for these gas molecules through increasing the containing-nitrogen functional groups on biochar. However, most of the nitrogen doping methods currently studied in this field are traditional high-temperature heat treatment methods, which have similar drawbacks to acid and alkali activation processes. Other some modification methods such as plasma discharge, ultraviolet radiation, microwave radiation, and so on may be potential alternatives because they possess relatively lower energy consumption or cleaner process. Besides, codoping of oxygen, phosphorus, sulfur, and/or nitrogen may have good developing potential since they have been shown to achieve faster electron transfer, more alkaline carbon surfaces, and stronger affinity for acidic substances in many other fields, which is worth exploration.

(4) Existing research on sulfur-containing gaseous pollutants adsorption by biochar mainly focuses on the study of simple experiments and characterization analysis. There is not enough research on the adsorption mechanism, especially using various in situ analysis methods and quantum chemical calculation methods, which leads to insufficient in-depth mechanism revelation. Research on the use of biochar to adsorb COS is relatively scarce. At present, a large amount of biochar-derived porous carbons and modified porous carbons have been developed in many other gas adsorption fields, and thus it is necessary to conduct research and evaluation in the field of COS removal. In addition, it is necessary to study the simultaneous removal of several sulfur-containing gaseous pollutants pollutants due to their coexistence in many industrial gas streams, which may greatly reduce the costs of removal system. The activation and regeneration of biochar after adsorption are crucial for reducing adsorption costs and the post-treatment cost of waste adsorbent. However, current research in this field is still not systematic and in-depth enough, and more research should be invested in.

(5) Adsorption of H_2S on biochar can be divided into physical and chemical adsorption. The large surface area and pore volume of biochar can promote the physical adsorption of H_2S by van der Waals forces. The oxygen-containing functional groups on the biochar surface can promote the catalytic oxidation of H_2S to produce S^0 and sulfate, and the nitrogen-containing functional groups on biochar surface can promote the dissociation of H_2S to produce HS^- and H^+, which are then further oxidized to S^0 and sulfate. The metal oxides supported on biochar surface can react with H_2S to produce metal sulfide. Adsorption of SO_2 on biochar can be also divided into physical and chemical adsorption. During chemisorption of SO_2, the oxygen-containing functional groups and chemisorbed oxygen on biochar surface can provide oxygen composition for oxidation of SO_2.

https://doi.org/10.1021/acs.energyfuels.4c06274
Energy Fuels XXXX, XXX, XXX−XXX

Addition of nitrogen-containing functional groups (such as pyridine, pyrrole, etc.) on the biochar surface can raise surface alkalinity of biochar, change surface charge distribution and polarity, which can make SO_2 more easily oxidized to SO_4^{2-}, promoting adsorption of SO_2. The metal oxides on the biochar surface can react with SO_2 to form metal sulfate. In addition to physical adsorption, COS adsorption on biochar surface can be divided into two processes: hydrolysis and catalytic oxidation. In the hydrolysis process, basic groups (such as −OH, pyridine, pyranes, etc.) and various metal oxides can increase surface alkalinity of biochar and promote hydrolysis of COS to H_2S and CO_2. The producing H_2S is further oxidized to S^0 and sulfate by catalytic oxidation. In the catalytic oxidation process, various oxygen-containing functional groups, lattice oxygen, and chemisorbed oxygen can promote COS oxidation to produce SO_2 and CO. Subsequently, the producing SO_2 is further oxidized to sulfuric acid and sulfate.

9. CONCLUSION

Compared with other removal technologies, adsorption removal of sulfur-containing gaseous pollutants by biochar possesses a good development prospect owing to several advantages such as a simple and clean process, renewability of adsorbent, and cheap raw materials. However, scarce active functional groups and active sites on biochar and underdeveloped pore structure limit the development and application of biochar adsorption removal technology in this field. Activation and modification of biochar are one of the most effective ways to raise biochar surface active sites and active functional groups, and improve the pore structure of biochar. Common activation and modification methods mainly include acid/alkali activation, microwave activation, metal oxide modification, nitrogen doping modification, and some emerging modification methods. Among these activation and modification methods, photochemical modification technology has the advantages of a simple and clean process and low energy consumption, and especially it can simultaneously introduce oxygen-containing functional groups on the surface of carbon materials and improve the pore structure of carbon materials, showing superior development prospects.

AUTHOR INFORMATION

Corresponding Authors

Yangxian Liu − *School of Energy and Power Engineering, Jiangsu University, Zhenjiang 212013, China;* orcid.org/0000-0001-9069-4007; Email: liuyx1984@126.com, liuyx@ujs.edu.cn

Yan Wang − *School of Energy and Power Engineering, Jiangsu University, Zhenjiang 212013, China*; Email: yanwang198882@126.com

Authors

Zihan Xiao − *School of Energy and Power Engineering, Jiangsu University, Zhenjiang 212013, China*

Jianfeng Pan − *School of Energy and Power Engineering, Jiangsu University, Zhenjiang 212013, China*

Complete contact information is available at: https://pubs.acs.org/10.1021/acs.energyfuels.4c06274

Notes

The authors declare no competing financial interest.

Biographies

Zihan Xiao is a master's degree candidate majoring in energy and power engineering from the School of Energy and Power Engineering, Jiangsu University of China. He received a bachelor's degree in power engineering and engineering thermophysics from Nanjing Forestry University of China in 2023. Zihan Xiao is mainly engaged in the research of H_2S removal using biochar adsorption.

Yangxian Liu is a Professor from School of Energy and Power Engineering, Jiangsu University of China. He received a Ph.D. in power engineering and engineering thermophysics from Southeast University of China. Dr. Liu is mainly engaged in the research of air pollutants (e.g., SO_2, NO_x, heavy metals, H_2S, CO, etc.) and CO_2 removal technologies.

Jianfeng Pan is a Professor from School of Energy and Power Engineering, Jiangsu University of China. He received a Ph.D. in power engineering and engineering thermophysics from Jiangsu University of China. Dr. Pan is mainly engaged in the research of advanced combustion and pollution control technologies.

Yan Wang is an assistant research fellow majoring in Power Engineering and Engineering Thermophysics, Jiangsu University of China. She received a Ph.D. in power engineering and engineering thermophysics from Jiangsu University of China. Yan Wang is mainly engaged in the research of flue gas purification using oxidation and adsorption technologies.

ACKNOWLEDGMENTS

This research work is sponsored by the National Natural Science Foundation of China (No. 52176111), the Outstanding Youth Fund of Jiangsu Province (No. BK20240044), the Jiangsu Funding Program for Excellent Postdoctoral Talent (No. 2024ZB112), and the Postdoctoral Fellowship Program of CPSF (No. GZC20240616).

REFERENCES

(1) Wang, Y.; Liu, Y. X.; Wang, Z. H.; Wang, Z. L. A thermally activated double oxidants advanced oxidation system for gaseous H2S removal: Mechanism and kinetics. *Chemical Engineering Journal* **2022**, *434*, 134430.

(2) Cesar, R.; Marques, P. J. L.; Tavares, J. R. A.; Antunes, F. C.; Gonçalves, J. M.; Vicentini, R.; Cavallari, M. R.; Brandao, B.; Hunt, J. D.; Doubek, G.; et al. Biogas Refining: A Review on Advances in Metal-Oxide-Modified Activated Carbon for H2S and CO2 Removal. *Energy Fuels* **2025**, *39* (1), 39−71.

(3) Wang, Y.; Wang, Y.; Liu, Y. X. Fe2+/heat-coactivated PMS oxidation-absorption system for H2S removal from gas phase. *Sep. Purif. Technol.* **2022**, *286*, 120458.

(4) Jiang, D.; Su, L.; Ma, L.; Yao, N.; Xu, X.; Tang, H.; Li, X. Cu-Zn-Al mixed metal oxides derived from hydroxycarbonate precursors for H2S removal at low temperature. *Appl. Surf. Sci.* **2010**, *256* (10), 3216−3223.

(5) Zhang, J.; Zhao, X. Q.; Ren, W.; Zhou, P.; Dong, Y.; Wang, T.; Zhang, L. Q.; Ma, C. Y.; Wang, W. L. Effects of Cobalt-Doped Modification on the Catalytic Reduction of SO2 with CO over an Iron/BFS Catalyst. *Energy Fuels* **2021**, *35* (24), 20250−20271.

(6) Carabineiro, S. A. C.; Ramos, A. M.; Vital, J.; Loureiro, J. M.; Orfao, J. J. M.; Fonseca, I. M. Adsorption of SO_2 using vanadium and vanadium-copper supported on activated carbon. *Catal. Today* **2003**, *78* (1−4), 203−210.

(7) Li, X. K.; Han, J. R.; Liu, Y.; Dou, Z. H.; Zhang, T. A. Summary of research progress on industrial flue gas desulfurization technology. *Sep. Purif. Technol.* **2022**, *281*, 119849.

(8) van Thriel, C.; Schäper, M.; Kleinbeck, S.; Kiesswetter, E.; Blaszkewicz, M.; Golka, K.; Nies, E.; Raulf-Heimsoth, M.; Brüning, T. Sensory and pulmonary effects of acute exposure to sulfur dioxide (SO2). *Toxicol. Lett.* **2010**, *196* (1), 42−50.
(9) Ma, M. Y.; Li, C. M.; Li, Y. J.; Wang, C.; Gao, S. Q.; Ye, H. D.; Li, J. J.; Yu, J. Resource Utilization of Spent Activated Coke as an Efficient Materialfor Simultaneous Removal of COS and H2S. *Energy Fuels* **2022**, *36* (9), 4837−4846.
(10) Jin, H. K.; An, Z. Y.; Li, Q. C.; Duan, Y. Q.; Zhou, Z. H.; Sun, Z. K.; Duan, L. B. Catalysts of Ordered Mesoporous Alumina with a Large Pore Size for Low-Temperature Hydrolysis of Carbonyl Sulfide. *Energy Fuels* **2021**, *35* (10), 8895−8908.
(11) Wei, Z.; Zhang, X.; Zhang, F. L.; Xie, Q.; Zhao, S. Z.; Hao, Z. P. Boosting carbonyl sulfide catalytic hydrolysis performance over N-doped Mg-Al oxide derived from MgAl-layered double hydroxide. *Journal of Hazardous Materials* **2021**, *407*, 124546.
(12) Sun, Z.; Liu, J. P.; Sun, Z. Q. Synergistic decarbonization and desulfurization of blast furnace gas via a novel magnesium-molybdenum looping process. *Fuel* **2020**, *279*, 118418.
(13) Liu, Y. X.; Shi, S.; Wang, Z. H. A novel double metal ions-double oxidants coactivation system for NO and SO2 simultaneous removal. *Chemical Engineering Journal* **2022**, *432*, 134398.
(14) Wang, Y.; Liu, Y. X.; Xu, J. J. Separation of hydrogen sulfide from gas phase using Ce3+Mn2+ enhanced fenton-like oxidation system. *Chemical Engineering Journal* **2019**, *359*, 1486−1492.
(15) Liu, D. J.; Zhou, W. G.; Wu, J. CeO_2-La_2O_3/ZSM-5 sorbents for high-temperature H_2S removal. *Korean Journal of Chemical Engineering* **2016**, *33* (6), 1837−1845.
(16) Xu, J. H.; Li, C. L.; Liu, P.; He, D.; Wang, J. F.; Zhang, Q. Photolysis of low concentration H_2S under UV/VUV irradiation emitted from high frequency discharge electrodeless lamps. *Chemosphere* **2014**, *109*, 202−207.
(17) Huang, L.; Xia, L. Y.; Ge, X. X.; Jing, H. Y.; Dong, W. B.; Hou, H. G. Removal of H_2S from gas stream using combined plasma photolysis technique at atmospheric pressure. *Chemosphere* **2012**, *88* (2), 229−234.
(18) Yu, Y.; Zhang, T. T.; Zheng, L. Q.; Yu, J. Photocatalytic degradation of hydrogen sulfide using TiO_2 film under microwave electrodeless discharge lamp irradiation. *Chemical Engineering Journal* **2013**, *225*, 9−15.
(19) Cha, J. S.; Park, S. H.; Jung, S. C.; Ryu, C.; Jeon, J. K.; Shin, M. C.; Park, Y. K. Production and utilization of biochar: A review. *Journal of Industrial and Engineering Chemistry* **2016**, *40*, 1−15.
(20) Wang, D. P.; Jing, Z. Q.; Wang, Y. Q.; Liu, T. Y.; Zhang, B. H.; Wen, C. The novel magnetic adsorbent derived from MIL-100 (Fe) loading with bimetallic Cu and Mn oxides for efficient Hg0 removal from flue gas. *Journal of Cleaner Production* **2022**, *377*, 134384.
(21) Bhatt, P. M.; Belmabkhout, Y.; Assen, A. H.; Weselinski, L. J.; Jiang, H.; Cadiau, A.; Xue, D. X.; Eddaoudi, M. Isoreticular rare earth fcu-MOFs for the selective removal of H2S from CO2 containing gases. *Chemical Engineering Journal* **2017**, *324*, 392−396.
(22) Wu, P. J.; Wang, Y.; Liu, Y. X. Recent advances in heteroatom-doped porous carbon for adsorption of gaseous pollutants. *Chemical Engineering Journal* **2024**, *491*, 152142, .
(23) Li, Y.; Wang, Y.; Wu, P. J.; Liu, Y. X.; Xu, H.; Zhao, Y. C. Application of plasma technology in Hg0 removal from flue gas: Recent advances and future perspectives. *Sep. Purif. Technol.* **2024**, *336*, 126259, .
(24) Shi, S.; Liu, Y. X. Nitrogen-doped activated carbons derived from microalgae pyrolysis by-products by microwave/KOH activation for CO_2 adsorption. *Fuel* **2021**, *306*, 121762, .
(25) Chen, J.; Yang, J.; Hu, G. S.; Hu, X.; Li, Z. M.; Shen, S. W.; Radosz, M.; Fan, M. H. Enhanced CO2 Capture Capacity of Nitrogen-Doped Biomass-Derived Porous Carbons. *Acs Sustainable Chemistry & Engineering* **2016**, *4* (3), 1439−1445.
(26) Zhang, W.; Li, Y. J.; Ma, X. T.; Qian, Y. Q.; Wang, Z. Y. Simultaneous NO/CO2 removal performance of biochar/limestone in calcium looping process. *Fuel* **2020**, *262*, 116428, .
(27) Iberahim, N.; Sethupathi, S.; Bashir, M. J. K.; Kanthasamy, R.; Ahmad, T. Evaluation of oil palm fiber biochar and activated biochar for sulphur dioxide adsorption. *Sci. Total Environ.* **2022**, *805*, 150421.
(28) Ning, Z. F.; Xu, B.; Zhong, W. Z.; Liu, C.; Qin, X.; Feng, W. B.; Zhu, L. Preparation of phosphoric acid modified antibiotic mycelial residues biochar: Loading of nano zero-valent iron and promotion on biogas production. *Bioresour. Technol.* **2022**, *348*, 126801, .
(29) Gwenzi, W.; Chaukura, N.; Wenga, T.; Mtisi, M. Biochars as media for air pollution control systems: Contaminant removal, applications and future research directions. *Sci. Total Environ.* **2021**, *753*, 142249, .
(30) Bamdad, H.; Hawboldt, K.; MacQuarrie, S. A review on common adsorbents for acid gases removal: Focus on biochar. *Renewable & Sustainable Energy Reviews* **2018**, *81*, 1705−1720.
(31) Sun, M. H.; Wang, X. Z.; Zhao, Z. B.; Qiu, J. S. Review of H_2S selective oxidation over carbon-based materials at low temperature: from pollutant to energy storage materials. *New Carbon Materials* **2022**, *37* (4), 675−690.
(32) Wei, D.; Wu, X. Q.; Guo, L.; Chen, J. L.; Wang, Y.; Yang, J.; Wu, L. Y.; Chen, Y. Research progress of carbonyl sulfide removal from blast furnace gas by porous materials. *Journal of Environmental Chemical Engineering* **2023**, *11* (3), 109606, .
(33) Xu, Q.; Liang, M.; Xu, W.; Huang, D. Advances in Mechanism and Influencing Factors Affecting Hydrogen Sulfide Adsorption by Biochar. *Environmental Science* **2021**, *42* (11), 5086−5099.
(34) Shang, G.; Shen, G.; Liu, L.; Chen, Q.; Xu, Z. Kinetics and mechanisms of hydrogen sulfide adsorption by biochars. *Bioresour. Technol.* **2013**, *133*, 495−499.
(35) Sun, Y.; Yang, G.; Zhang, L.; Sun, Z. Preparation of high performance H 2 S removal biochar by direct fluidized bed carbonization using potato peel waste. *Process Safety and Environmental Protection* **2017**, *107*, 281−288.
(36) Yang, G.; Sun, Y.; Zhang, J. P.; Wen, C. Fast carbonization using fluidized bed for biochar production from reed black liquor: optimization for H2S removal. *Environmental Technology* **2016**, *37* (19), 2447−2456.
(37) Sun, Y.; Zhang, J. P.; Wen, C.; Zhang, L. An enhanced approach for biochar preparation using fluidized bed and its application for H2S removal. *Chemical Engineering and Processing-Process Intensification* **2016**, *104*, 1−12.
(38) Yuan, W. X.; Bandosz, T. J. Removal of hydrogen sulfide from biogas on sludge-derived adsorbents. *Fuel* **2007**, *86* (17−18), 2736−2746.
(39) Bandosz, T. J. On the adsorption/oxidation of hydrogen sulfide on activated carbons at ambient temperatures. *J. Colloid Interface Sci.* **2002**, *246* (1), 1−20.
(40) Han, X.; Chen, H.; Liu, Y.; Pan, J. Study on removal of gaseous hydrogen sulfide based on macroalgae biochars. *Journal of Natural Gas Science and Engineering* **2020**, *73*, 103068, .
(41) Sawalha, H.; Maghalseh, M.; Qutaina, J.; Junaidi, K.; Rene, E. R. Removal of hydrogen sulfide from biogas using activated carbon synthesized from different locally available biomass wastes-a case study from Palestine. *Bioengineered* **2020**, *11* (1), 607−618.
(42) Sethupathi, S.; Zhang, M.; Rajapaksha, A. U.; Lee, S. R.; Nor, N. M.; Mohamed, A. R.; Al-Wabel, M.; Lee, S. S.; Ok, Y. S. Biochars as Potential Adsorbers of CH_4, CO_2 and H_2S. *Sustainability* **2017**, *9* (1), 121, .
(43) Oliveira, F. R.; Surendra, K. C.; Jaisi, D. P.; Lu, H.; Unal-Tosun, G.; Sung, S.; Khanal, S. K. Alleviating sulfide toxicity using biochar during anaerobic treatment of sulfate-laden wastewater. *Bioresour. Technol.* **2020**, *301*, 122711.
(44) Xu, X.; Cao, X.; Zhao, L.; Sun, T. Comparison of sewage sludge- and pig manure-derived biochars for hydrogen sulfide removal. *Chemosphere* **2014**, *111*, 296−303.
(45) Xu, X. Y.; Huang, D. X.; Zhao, L.; Kan, Y.; Cao, X. D. Role of Inherent Inorganic Constituents in SO_2 Sorption Ability of Biochars Derived from Three Biomass Wastes. *Environ. Sci. Technol.* **2016**, *50* (23), 12957−12965.

https://doi.org/10.1021/acs.energyfuels.4c06274
Energy Fuels XXXX, XXX, XXX−XXX

(46) Serafin, J.ła.; Ouzzine, M.; Cruz, O. F.; Srenscek-Nazzal, J.; Campello Gomez, I.; Azar, F.-Z.; Rey Mafull, C. A.; Hotza, D.; Rambo, C. R. Conversion of fruit waste-derived biomass to highly microporous activated carbon for enhanced CO2 capture. *Waste Management* **2021**, *136*, 273−282.
(47) Xiang, S.; Zhang, Z.; Xing, X.; She, Y.; Guo, S. Research progress of activated carbon for desulfurization and denitrification of sintering flue gas. *Journal of Iron and Steel Research* **2023**, *35* (3), 233−246.
(48) Wang, X. H.; Cheng, H. R.; Ye, G. Z.; Fan, J.; Yao, F.; Wang, Y. Q.; Jiao, Y. J.; Zhu, W. F.; Huang, H. M.; Ye, D. Q. Key factors and primary modification methods of activated carbon and their application in adsorption of carbon-based gases: A review. *Chemosphere* **2022**, *287*, 131995, .
(49) Li, Y.; Wang, Y.; Dou, Z. F.; Liu, Y. X. Removal of gaseous Hg0 using biomass porous carbons modified by an environmental-friendly photochemical technique. *Chemical Engineering Journal* **2023**, *457*, 141152, .
(50) Wang, Y.; Ma, C.; Liu, Y. X. Oxidation absorption of nitric oxide from flue gas using biochar-activated peroxydisulfate technology. *Fuel* **2023**, *337*, 127189, .
(51) Zhou, M. L.; Xu, Y.; Luo, G. Q.; Zhang, Q. Z.; Du, L.; Cui, X. W.; Li, Z. H. Facile synthesis of phosphorus-doped porous biochars for efficient removal of elemental mercury from coal combustion flue gas. *Chemical Engineering Journal* **2022**, *432*, 134440, .
(52) Wang, Y.; Ma, C.; Kong, D. X.; Lian, L. Q.; Liu, Y. X. Review on application of algae-based biochars in environmental remediation: Progress, challenge and perspectives. *Journal of Environmental Chemical Engineering* **2023**, *11* (6), 111263, .
(53) Li, Y.; Wang, Y.; Liu, Y. X.; Zhao, Y. C. Clean Modification of Carbon-Based Materials Using Hydroxyl Radicals and Preliminary Study on Gaseous Elemental Mercury Removal. *Energy Fuels* **2023**, *37* (8), 5953−5960.
(54) Guo, W. P.; Yao, X.; Chen, Z.; Liu, T.; Wang, W.; Zhang, S. J.; Xian, J. Q.; Wang, Y. H. Recent advance on application of biochar in remediation of heavy metal contaminated soil: Emphasis on reaction factor, immobilization mechanism and functional modification. *Journal of Environmental Management* **2024**, *371*, 123212, .
(55) Liang, D. Z.; Li, C. B.; Chen, H. B.; Sormo, E.; Cornelissen, G.; Gao, Y. R.; Reguyal, F.; Sarmah, A.; Ippolito, J.; Kammann, C.; et al. A critical review of biochar for the remediation of PFAS-contaminated soil and water. *Sci. Total Environ.* **2024**, *951*, 174962, .
(56) Bazan-Wozniak, A.; Nowicki, P.; Pietrzak, R. The influence of activation procedure on the physicochemical and sorption properties of activated carbons prepared from pistachio nutshells for removal of NO2 /H2S gases and dyes. *Journal of Cleaner Production* **2017**, *152*, 211−222.
(57) Heidarinejad, Z.; Dehghani, M. H.; Heidari, M.; Javedan, G.; Ali, I.; Sillanpää, M. Methods for preparation and activation of activated carbon: a review. *Environmental Chemistry Letters* **2020**, *18* (2), 393−415.
(58) Ello, A. S.; de Souza, L. K. C.; Trokourey, A.; Jaroniec, M. Coconut shell-based microporous carbons for CO2 capture. *Microporous Mesoporous Mater.* **2013**, *180*, 280−283.
(59) González, A. S.; Plaza, M. G.; Rubiera, F.; Pevida, C. Sustainable biomass-based carbon adsorbents for post-combustion CO2 capture. *Chemical Engineering Journal* **2013**, *230*, 456−465.
(60) Wen, C.; Liu, T. Y.; Wang, D. P.; Wang, Y. Q.; Chen, H. P.; Luo, G. Q.; Zhou, Z. J.; Li, C. K.; Xu, M. H. Biochar as the effective adsorbent to combustion gaseous pollutants: Preparation, activation, functionalization and the adsorption mechanisms. *Prog. Energy Combust. Sci.* **2023**, *99*, 101098, .
(61) Zhao, Z. P.; Wang, B.; Theng, B. K. G.; Lee, X. Q.; Zhang, X. Y.; Chen, M.; Xu, P. Removal performance, mechanisms, and influencing factors of biochar for air pollutants: a critical review. *Biochar* **2022**, *4* (1). DOI: 10.1007/s42773-022-00156-z.
(62) Guo, J.; Luo, Y.; Lua, A. C.; Chi, R.-a.; Chen, Y.-l.; Bao, X.-t.; Xiang, S.-x. Adsorption of hydrogen sulphide (H2S) by activated carbons derived from oil-palm shell. *Carbon* **2007**, *45* (2), 330−336.
(63) Chen, H.; Han, X.; Liu, Y. Gaseous Hydrogen Sulfide Removal Using Macroalgae Biochars Modified Synergistically by H2SO4/H2O2. *Chem. Eng. Technol.* **2021**, *44* (4), 698−709.
(64) Guo, J.; Lua, A. C. Adsorption of sulphur dioxide onto activated carbon prepared from oil-palm shells with and without pre-impregnation. *Sep. Purif. Technol.* **2003**, *30* (3), 265−273.
(65) Yavuz, R.; Akyildiz, H.; Karatepe, N.; Çetinkaya, E. Influence of preparation conditions on porous structures of olive stone activated by H3PO4. *Fuel Process. Technol.* **2010**, *91* (1), 80−87.
(66) Liu, X.; Liu, L.; Osaka, Y.; Huang, H.; He, Z.; Bai, Y.; Li, S.; Li, J.; Huhetaoli. Study on desulfurization performance of MnO2-based activated carbon from waste coconut shell for diesel emissions control. *Journal of Material Cycles and Waste Management* **2018**, *20* (3), 1499−1506.
(67) Wang, S.; Nam, H.; Nam, H. Preparation of activated carbon from peanut shell with KOH activation and its application for H2S adsorption in confined space. *Journal of Environmental Chemical Engineering* **2020**, *8* (2), 103683, .
(68) Wang, S.; Nam, H.; Gebreegziabher, T. B.; Nam, H. Adsorption of acetic acid and hydrogen sulfide using NaOH impregnated activated carbon for indoor air purification. *Engineering Reports* 2020, *2* (5).
(69) Singh, G.; Ruban, A. M.; Geng, X.; Vinu, A. Recognizing the potential of K-salts, apart from KOH, for generating porous carbons using chemical activation. *Chemical Engineering Journal* **2023**, *451*, 139045, .
(70) Li, K.; Ruan, H.; Ning, P.; Wang, C.; Sun, X.; Song, X.; Han, S. Preparation of walnut shell-based activated carbon and its properties for simultaneous removal of H2S, COS and CS2 from yellow phosphorus tail gas at low temperature. *Res. Chem. Intermed.* **2018**, *44* (2), 1209−1233.
(71) Kamran, U.; Park, S. J. Chemically modified carbonaceous adsorbents for enhanced CO_2 capture: A review. *Journal of Cleaner Production* **2021**, *290*, 125776, .
(72) Zeng, F.; Liao, X. F.; Hu, H.; Liao, L. Effect of potassium hydroxide activation in the desulfurization process of activated carbon prepared by sewage sludge and corn straw. *J. Air Waste Manage. Assoc.* **2018**, *68* (3), 255−264.
(73) Cao, Q.; Xie, K. C.; Lv, Y. K.; Bao, W. R. Process effects on activated carbon with large specific surface area from corn cob. *Bioresour. Technol.* **2006**, *97* (1), 110−115.
(74) Ma, C.; Zhao, Y.; Chen, H.; Liu, Y.; Huang, R.; Pan, J. Biochars derived from by-products of microalgae pyrolysis for sorption of gaseous H_2S. *Journal of Environmental Chemical Engineering* **2022**, *10* (3), 107370.
(75) Bagreev, A.; Bandosz, T. J. A role of sodium hydroxide in the process of hydrogen sulfide adsorption/oxidation on caustic-impregnated activated carbons. *Ind. Eng. Chem. Res.* **2002**, *41* (4), 672−679.
(76) Bashkova, S.; Bagreev, A.; Locke, D. C.; Bandosz, T. J. Adsorption of SO2 on sewage sludge-derived materials. *Environ. Sci. Technol.* **2001**, *35* (15), 3263−3269.
(77) Lee, Y. W.; Park, J. W.; Choung, J. H.; Choi, D. K. Adsorption characteristics of SO2 on activated carbon prepared from coconut shell with potassium hydroxide activation. *Environ. Sci. Technol.* **2002**, *36* (5), 1086−1092.
(78) Atanes, E.; Nieto-Márquez, A.; Cambra, A.; Ruiz-Pérez, M. C.; Fernández-Martínez, F. Adsorption of SO2 onto waste cork powder-derived activated carbons. *Chemical Engineering Journal* **2012**, *211−212*, 60−67.
(79) Braghiroli, F. L.; Bouafif, H.; Koubaa, A. Enhanced SO2 adsorption and desorption on chemically and physically activated biochar made from wood residues. *Industrial Crops and Products* **2019**, *138*, 111456, .
(80) Nguyen-Thanh, D.; Bandosz, T. J. Activated carbons with metal containing bentonite binders as adsorbents of hydrogen sulfide. *Carbon* **2005**, *43* (2), 359−367.
(81) Berhe Gebreegziabher, T.; Wang, S.; Nam, H. Adsorption of H_2S, NH_3 and TMA from indoor air using porous corncob activated

https://doi.org/10.1021/acs.energyfuels.4c06274
Energy Fuels XXXX, XXX, XXX−XXX

carbon: Isotherm and kinetics study. *Journal of Environmental Chemical Engineering* **2019**, *7* (4), 103234, .
(82) Nowicki, P.; Skibiszewska, P.; Pietrzak, R. Hydrogen sulphide removal on carbonaceous adsorbents prepared from coffee industry waste materials. *Chemical Engineering Journal* **2014**, *248*, 208−215.
(83) Menezes, R.; Moura, K. O.; de Lucena, S. M. P.; Azevedo, D. C. S.; Bastos-Neto, M. Insights on the Mechanisms of H_2S Retention at Low Concentration on Impregnated Carbons. *Ind. Eng. Chem. Res.* **2018**, *57* (6), 2248−2257.
(84) Sitthikhankaew, R.; Chadwick, D.; Assabumrungrat, S.; Laosiripojana, N. Performance of Sodium-Impregnated Activated Carbons toward Low and High Temperature H_2S Adsorption. *Chem. Eng. Commun.* **2014**, *201* (2), 257−271.
(85) Lin, Q.; Zhang, J.; Yin, L.; Liu, H.; Zuo, W.; Tian, Y. Relationship between heavy metal consolidation and H(2)S removal by biochar from microwave pyrolysis of municipal sludge: effect and mechanism. *Environ. Sci. Pollut Res. Int.* **2021**, *28* (22), 27694−27702.
(86) Dou, Z.; Chen, H.; Liu, Y.; Huang, R.; Pan, J. Removal of gaseous H2S using microalgae porous carbons synthesized by thermal/microwave KOH activation. *Journal of the Energy Institute* **2022**, *101*, 45−55.
(87) Cui, S. B.; Zhao, Y.; Liu, Y. X.; Huang, R. K.; Pan, J. F. Preparation of Straw Porous Biochars by Microwave-Assisted KOH Activation for Removal of Gaseous H2S. *Energy Fuels* **2021**, *35* (22), 18592−18603.
(88) Xu, S.; Deng, W.; Hu, M.; Chen, G.; Zhou, P.; Li, F.; Su, Y. Preparation of activated sludge char through microwave-assisted one-step pyrolysis and activation for gaseous H2S removal. *Chemical Engineering and Processing - Process Intensification* **2022**, *181*, 109175, .
(89) Mohamad Nor, N.; Sukri, M. F. F.; Mohamed, A. R. Development of high porosity structures of activated carbon via microwave-assisted regeneration for H2S removal. *Journal of Environmental Chemical Engineering* **2016**, *4* (4, Part B), 4839−4845.
(90) Kazmierczak-Razna, J.; Gralak-Podemska, B.; Nowicki, P.; Pietrzak, R. The use of microwave radiation for obtaining activated carbons from sawdust and their potential application in removal of NO2 and H2S. *Chemical Engineering Journal* **2015**, *269*, 352−358.
(91) Zhu, M.; Hu, M.; Deng, W.; Su, Y. Preparation of red mud-modified sludge char through microwave-assisted one-step pyrolysis and steam activation and its adsorption properties for hydrogen sulfide. *Chemosphere* **2024**, *368*, 143723.
(92) Zhang, L.; Cui, L.; Wang, Z.; Dong, Y. Modification of Activated Carbon Using Microwave Radiation and Its Effects on the Adsorption of SO_2. *J. Chem. Eng. Jpn.* **2016**, *49* (1), 52−59.
(93) Fengrui, J.; Zhou, L.; Engang, W.; Jicheng, H.; Hui, D.; Guangxin, L.; Weiwei, J. Preparation and SO_2 Adsorption Behavior of Coconut ShellBased Activated Carbon via Microwave-Assisted Oxidant Activation. *China Petroleum Processing and Petrochemical Technology* **2018**, *20* (1), 67−74.
(94) Sakanishi, K.; Wu, Z.; Matsumura, A.; Saito, I.; Hanaoka, T.; Minowa, T.; Tada, M.; Iwasaki, T. Simultaneous removal of H2S and COS using activated carbons and their supported catalysts. *Catal. Today* **2005**, *104* (1), 94−100.
(95) Wang, H.; Chen, S.; Zhang, Y. Study on adsorption of carbonyl sulfide by KOH modified activated carbon and regeneration performance. *Xiandai Huagong/Modern Chemical Industry* **2019**, *39* (01), 128−132.
(96) Ruan, H. Simultaneous removal of H_2S, COS, and CS_2 with tobacco stem biochar carrier catalyst. **2017**. https://kns.cnki.net/KCMS/detail/detail.aspx?filename=1017221287.nh&dbname=CMFDTEMP.
(97) Shah, M. S.; Tsapatsis, M.; Siepmann, J. I. Hydrogen Sulfide Capture: From Absorption in Polar Liquids to Oxide, Zeolite, and Metal-Organic Framework Adsorbents and Membranes (vol 117, pg 9755, 2017). *Chem. Rev.* **2018**, *118* (4), 2297−2297.
(98) Zhang, X. Y.; Cui, L.; An, D. H.; Fu, J. P.; Liu, J.; Dong, Y. H2S-Selective Catalytic Oxidation to Sulfur over Iron Oxide Sorbent Supported on Semi-Coke. *Energy Fuels* **2020**, *34* (2), 2315−2322.
(99) Xue, M.; Chitrakar, R.; Sakane, K.; Ooi, K. Screening of adsorbents for removal of H2S at room temperature. *Green Chem.* **2003**, *5* (5), 529−534.
(100) Livraghi, S.; Paganini, M. C.; Giamello, E. SO2 reactivity on the MgO and CaO surfaces: A CW-EPR study of oxo-sulphur radical anions. *J. Mol. Catal. A: Chem.* **2010**, *322* (1−2), 39−44.
(101) Liu, H. P.; Zhang, Q.; Yang, H. Y.; Wu, Y. N.; Chen, J. C.; Hu, S. Effect of Metal Oxides and Smelting Dust on SO_2 Conversion to SO3. *Atmosphere* **2021**, *12* (6), 734, .
(102) Gupta, N. K.; Rajput, K.; Achary, S. N.; Kim, E. J.; Mehta, B. R.; Roy, D. R.; Kim, K. S. Hydrogen Sulfide Gas Capture by Discarded Zn-MnO2 Alkaline Batteries in Ambient Conditions. *Energy Fuels* **2024**, *38* (8), 7431−7435.
(103) Montes, D.; Tocuyo, E.; González, E.; Rodríguez, D.; Solano, R.; Atencio, R.; Ramos, M. A.; Moronta, A. Reactive H2S chemisorption on mesoporous silica molecular sieve-supported CuO or ZnO. *Microporous Mesoporous Mater.* **2013**, *168*, 111−120.
(104) Yang, J. H. Hydrogen sulfide removal technology: A focused review on adsorption and catalytic oxidation. *Korean Journal of Chemical Engineering* **2021**, *38* (4), 674−691.
(105) Giannakoudakis, D. A.; Bandosz, T. J. Zinc (hydr)oxide/graphite oxide/AuNPs composites: Role of surface features in H2S reactive adsorption. *J. Colloid Interface Sci.* **2014**, *436*, 296−305.
(106) Tang, X. G.; Wu, P. J.; Wang, Y.; Liu, Y. X. Recent advances in heavy metal poisoning mechanism and regeneration methods of selective catalytic reduction (SCR) denitration catalyst. *Fuel* **2024**, *355*, 129429, .
(107) He, Z. H.; Wang, Y.; Liu, Y. X.; Lian, L. Q.; Kong, D. X.; Zhao, Y. C. Recent advances in sulfur poisoning of selective catalytic reduction (SCR) denitration catalysts. *Fuel* **2024**, *365*, 131126, .
(108) Yang, C.; Florent, M.; de Falco, G.; Fan, H.; Bandosz, T. J. $ZnFe_2O_4$/activated carbon as a regenerable adsorbent for catalytic removal of H_2S from air at room temperature. *Chemical Engineering Journal* **2020**, *394*, 124906, .
(109) Yang, W.; Adewuyi, Y. G.; Hussain, A.; Liu, Y. X. Recent developments on gas-solid heterogeneous oxidation removal of elemental mercury from flue gas. *Environmental Chemistry Letters* **2019**, *17* (1), 19−47.
(110) Yin, M. X.; Pillai, S. C.; Bolan, N.; Wang, H. L.; Yin, H. L.; Wu, Z. H.; Zheng, Y.; Zhao, L.; Fan, F. Y.; Hou, H. Low temperature selective catalytic oxidation of H2S: Influencing factors, mechanisms and regeneration. *Chemical Engineering Journal* **2024**, *479*, 147854, .
(111) Cui, S. B.; Zhao, Y.; Liu, Y. X.; Pan, J. F. Preparation of copper-based biochar adsorbent with outstanding H2S adsorption capacity and study on H2S removal. *Journal of the Energy Institute* **2022**, *105*, 481−490.
(112) Choudhury, A.; Lansing, S. Biochar addition with Fe impregnation to reduce H2S production from anaerobic digestion. *Bioresour. Technol.* **2020**, *306*, 123121.
(113) Chen, J. L.; Huang, L. H.; Sun, L. M.; Zhu, X. F. Desulfurization Performance of MgO/ Rice Straw Biochar Adsorbent Prepared by Co-precipitation/ Calcination Route. *Bioresources* **2020**, *15* (3), 4738−4752.
(114) Macías-Pérez, M. C.; Lillo-Ródenas, M. A.; Bueno-López, A.; Salinas-Martínez de Lecea, C.; Linares-Solano, A. SO2 retention on CaO/activated carbon sorbents. Part II: Effect of the activated carbon support. *Fuel* **2008**, *87* (12), 2544−2550.
(115) Balsamo, M.; Cimino, S.; de Falco, G.; Erto, A.; Lisi, L. ZnO-CuO supported on activated carbon for H2S removal at room temperature. *Chemical Engineering Journal* **2016**, *304*, 399−407.
(116) Wang, Z.; Huang, J.; Zhong, Y.; Hu, W.; Xie, D.; Zhao, C.; Qiao, Y. Copper supported on activated carbon from hydrochar of pomelo peel for efficient H_2S removal at room temperature: Role of copper valance, humidity and oxygen. *Fuel* **2022**, *319*, 123774, .
(117) Wang, S.; Nam, H.; Lee, D.; Nam, H. H2S gas adsorption study using copper impregnated on KOH activated carbon from coffee residue for indoor air purification. *Journal of Environmental Chemical Engineering* **2022**, *10* (6), 108797, .

https://doi.org/10.1021/acs.energyfuels.4c06274
Energy Fuels XXXX, XXX, XXX−XXX

(118) Zhao, Y.; Liu, Y. Preparation of hydrogen sulfide adsorbent derived from spent Fenton-like reagent modified biochar and its removal characteristics for hydrogen sulfide. *Fuel Process. Technol.* **2022**, *238*, 107495, .
(119) Li, F.; Wei, J.; Yang, Y.; Yang, G. H.; Lei, T. Preparation of Sorbent Loaded with Nano-CuO for Room Temperature to Remove of Hydrogen Sulfide. *Applied Mechanics and Materials* **2013**, *475*−*476*, 1329−1333.
(120) Yang, C.; Wang, J.; Fan, H. L.; Ju, S. G.; Mi, J.; Huo, C. Contributions of tailored oxygen vacancies in ZnO/Al_2O_3 composites to the enhanced ability for H_2S removal at room temperature. *Fuel* **2018**, *215*, 695−703.
(121) Li, L.; Sun, T. H.; Shu, C. H.; Zhang, H. B. Low temperature H2S removal with 3-D structural mesoporous molecular sieves supported ZnO from gas stream. *Journal of Hazardous Materials* **2016**, *311*, 142−150.
(122) Hernández, S. P.; Chiappero, M.; Russo, N.; Fino, D. A novel ZnO-based adsorbent for biogas purification in H2 production systems. *Chemical Engineering Journal* **2011**, *176*, 272−279.
(123) Zhang, J. J.; Wang, W. Y.; Shen, L. P.; Wang, G. J.; Song, H. Synthesis and characterization of MnxOy-ZnxOy/AC adsorbents for adsorptive removal of H2S from natural gas. *Adsorption Science & Technology* **2016**, *34* (4−5), 331−341.
(124) Choudhury, A.; Lansing, S. Adsorption of hydrogen sulfide in biogas using a novel iron-impregnated biochar scrubbing system. *Journal of Environmental Chemical Engineering* **2021**, *9* (1), 104837, .
(125) Wang, J. C.; Ju, F. L.; Han, L. N.; Qin, H. C.; Hu, Y. F.; Chang, L. P.; Bao, W. R. Effect of Activated Carbon Supports on Removing H2S from Coal-Based Gases using Mn-Based Sorbents. *Energy Fuels* **2015**, *29* (2), 488−495.
(126) Lau, L. C.; Nor, N. M.; Lee, K. T.; Mohamed, A. R. Hydrogen sulfide removal using CeO2/NaOH/PSAC: Effect of preparation parameters. *Journal of Environmental Chemical Engineering* **2018**, *6* (1), 386−394.
(127) Xu, W.; Adewuyi, Y. G.; Liu, Y. X.; Wang, Y. Removal of elemental mercury from flue gas using CuOx and CeO2 modified rice straw chars enhanced by ultrasound. *Fuel Process. Technol.* **2018**, *170*, 21−31.
(128) Zhang, J. J.; Shen, L. P.; Song, H.; Wang, L.; Wang, X. Q.; Dong, L. Research on adsorptive desulfurization of H2S from natural gas over MnxOy-CoxOy supported on activated carbon. *Adsorption Science & Technology* **2016**, *34* (2−3), 134−143.
(129) Yuan, Y.; Huang, L.; Zhang, T. C.; Ouyang, L.; Yuan, S. One-step synthesis of $ZnFe_2O_4$-loaded biochar derived from leftover rice for high-performance H_2S removal. *Sep. Purif. Technol.* **2021**, *279*, 119686, .
(130) Yuan, Y.; Huang, L.; Yılmaz, M.; Zhang, T. C.; Wang, Y.; Yuan, S. $MgFe_2O_4$-loaded N-doped biochar derived from waste cooked rice for efficient low-temperature desulfurization of H2S. *Fuel* **2023**, *339*, 127385, .
(131) Yuan, Y.; Huang, L.; Zhang, T. C.; Wang, Y.; Yuan, S. $CaCO_3$-ZnO loaded scrap rice-derived biochar for H2S removal at room-temperature: Characterization, performance and mechanism. *Fuel Process. Technol.* **2023**, *249*, 107846, .
(132) Li, L.; Zhang, H. B.; Zhou, P.; Meng, X. L.; Liu, L. Z.; Jia, J. P.; Sun, T. H. Three dimensional ordered macroporous zinc ferrite composited silica sorbents with promotional desulfurization and regeneration activity at mid-high temperature. *Appl. Surf. Sci.* **2019**, *470*, 177−186.
(133) Chen, S.; Guo, Y.; Zhang, J.; Guo, Y.; Liang, X. $CuFe_2O_4$/activated carbon adsorbents enhance H2S adsorption and catalytic oxidation from humidified air at room temperature. *Chemical Engineering Journal* **2022**, *431*, 134097.
(134) Tseng, H.-H.; Wey, M.-Y. Study of SO2 adsorption and thermal regeneration over activated carbon-supported copper oxide catalysts. *Carbon* **2004**, *42* (11), 2269−2278.
(135) Fan, L.; Chen, J.; Guo, J.; Jiang, X.; Jiang, W. Influence of manganese, iron and pyrolusite blending on the physiochemical properties and desulfurization activities of activated carbons from walnut shell. *Journal of Analytical and Applied Pyrolysis* **2013**, *104*, 353−360.
(136) Sumathi, S.; Bhatia, S.; Lee, K. T.; Mohamed, A. R. Selection of best impregnated palm shell activated carbon (PSAC) for simultaneous removal of SO2 and NOx. *J. Hazard Mater.* **2010**, *176* (1−3), 1093−1096.
(137) Liang, S. J.; Liu, F. J.; Jiang, L. L. Recent advances on nitrogen-doped metal-free materials for the selective catalytic oxidation of hydrogen sulfide. *Current Opinion in Green and Sustainable Chemistry* **2020**, *25*, 100361, .
(138) Seredych, M.; Bandosz, T. J. Desulfurization of digester gas on wood-based activated carbons modified with nitrogen: Importance of surface chemistry. *Energy Fuels* **2008**, *22* (2), 850−859.
(139) Strelko, V. V.; Kuts, V. S.; Thrower, P. A. On the mechanism of possible influence of heteroatoms of nitrogen, boron and phosphorus in a carbon matrix on the catalytic activity of carbons in electron transfer reactions. *Carbon* **2000**, *38* (10), 1499−1503.
(140) Seredych, M.; Bandosz, T. J. Role of microporosity and nitrogen functionality on the surface of activated carbon in the process of desulfurization of digester gas. *J. Phys. Chem. C* **2008**, *112* (12), 4704−4711.
(141) Bashkova, S.; Baker, F. S.; Wu, X. X.; Armstrong, T. R.; Schwartz, V. Activated carbon catalyst for selective oxidation of hydrogen sulphide: On the influence of pore structure, surface characteristics, and catalytically-active nitrogen. *Carbon* **2007**, *45* (6), 1354−1363.
(142) Zhang, X.; Zhang, S.; Zhang, J.; Li, G.; Zheng, H.; Shao, J.; Zhang, S.; Yang, H.; Chen, H. Enhanced SO2 adsorption performance on nitrogen-doped biochar: Insights from generalized two-dimensional correlation infrared spectroscopy. *Fuel* **2023**, *354*, 129266, .
(143) Setiawan, H.; Sakamoto, M.; Fujisaki, T.; Lyth, S. M.; Shiratori, Y. Development of a sustainable nitrogen-doped biochar desulfurizer for solid oxide fuel cell systems. *Biomass and Bioenergy* **2022**, *167*, 106631, .
(144) Nor, N. M.; Chung, L. L.; Mohamed, A. R. Development of microwave-assisted nitrogen-modified activated carbon for efficient biogas desulfurization: a practical approach. *Environ. Sci. Pollut Res. Int.* **2023**, *30* (7), 17129−17148.
(145) Hu, W.; Huang, J.; Wang, J.; Xie, D.; Wang, Z.; Qiao, Y.; Xu, M. Benign-by-design N-doped activated carbon from wasted aqueous assisted hydrochar of leftover rice for efficient H2S removal. *Fuel* **2024**, *358*, 130233, .
(146) Hervy, M.; Minh, D. P.; Gérente, C.; Weiss-Hortala, E.; Nzihou, A.; Villot, A.; Le Coq, L. H2S removal from syngas using wastes pyrolysis chars. *Chemical Engineering Journal* **2018**, *334*, 2179−2189.
(147) Feng, J. Y.; Jia, L. J.; Wang, F.; Sun, X.; Ning, P.; Wang, C.; Li, Y.; Li, K. Urea-modified Cu-based materials: Highly efficient and support-free adsorbents for removal of H2S in an anaerobic and dry environment. *Chemical Engineering Journal* **2023**, *451*, 138815, .
(148) Chen, L.; Yuan, J.; Li, T.; Jiang, X.; Ma, S.; Cen, W.; Jiang, W. A regenerable N-rich hierarchical porous carbon synthesized from waste biomass for H_2S removal at room temperature. *Science of The Total Environment* **2021**, *768*, 144452, .
(149) Wu, J.; Chen, W.; Chen, L.; Jiang, X. Super-high N-doping promoted formation of sulfur radicals for continuous catalytic oxidation of H2S over biomass derived activated carbon. *J. Hazard Mater.* **2022**, *424* (Pt D), 127648.
(150) Li, K.; Niu, X.; Zhou, L.; Zheng, Y.; Lin, Z.; Liu, M. Renewable N-doped biochars for H2S removal at room temperature: Characterization, performance and mechanism. *Industrial Crops and Products* **2025**, *225*, 120416.
(151) Rezaei, F.; Rownaghi, A. A.; Monjezi, S.; Lively, R. P.; Jones, C. W. SOx/NOx Removal from Flue Gas Streams by Solid Adsorbents: A Review of Current Challenges and Future Directions. *Energy Fuels* **2015**, *29* (9), 5467−5486.
(152) Li, D.; Chen, W.; Wu, J.; Jia, C. Q.; Jiang, X. The preparation of waste biomass-derived N-doped carbons and their application in

https://doi.org/10.1021/acs.energyfuels.4c06274
Energy Fuels XXXX, XXX, XXX−XXX

acid gas removal: focus on N functional groups. *Journal of Materials Chemistry A* **2020**, *8* (47), 24977−24995.
(153) Raymundo-Piñero, E.; Cazorla-Amorós, D.; de Lecea, C. S. M.; Linares-Solano, A. Factors controling the SO2 removal by porous carbons:: relevance of the SO2 oxidation step. *Carbon* **2000**, *38* (3), 335−344.
(154) Qu, Z. B.; Sun, F.; Liu, X.; Gao, J. H.; Qie, Z. P.; Zhao, G. B. The effect of nitrogen-containing functional groups on SO2 adsorption on carbon surface: Enhanced physical adsorption interactions. *Surf. Sci.* **2018**, *677*, 78−82.
(155) Zhang, X.; Zheng, H.; Li, G.; Gu, J.; Shao, J.; Zhang, S.; Yang, H.; Chen, H. Ammoniated and activated microporous biochar for enhancement of SO_2 adsorption. *Journal of Analytical and Applied Pyrolysis* **2021**, *156*, 105119, .
(156) Zhang, J.; Shao, J.; Huang, D.; Feng, Y.; Zhang, X.; Zhang, S.; Chen, H. Influence of different precursors on the characteristic of nitrogen-enriched biochar and SO_2 adsorption properties. *Chemical Engineering Journal* **2020**, *385*, 123932, .
(157) Wang, L.; Sha, L.; Zhang, S.; Cao, F.; Ren, X.; Levendis, Y. A. Preparation of activated coke by carbonization, activation, ammonization and thermal treatment of sewage sludge and waste biomass for SO_2 absorption applications. *Fuel Process. Technol.* **2022**, *231*, 107233, .
(158) Li, X.; Wang, X. Q.; Wang, L. L.; Yuan, L.; Ma, Y. X.; Xie, Y. B.; Xiong, Y. R.; Ning, P. Alkali-induced metal-based coconut shell biochar for efficient catalytic removal of H2S at a medium-high temperature in blast furnace gas with significantly enhanced S selectivity. *Sep. Purif. Technol.* **2023**, *306*, 122698, .
(159) Zhang, J.; Wang, L.; Song, H.; Song, H. Adsorption of low-concentration H2S on manganese dioxide-loaded activated carbon. *Res. Chem. Intermed.* **2015**, *41* (9), 6087−6104.
(160) Abriyani, D.; Ariyanto, T.; Prasetyo, I. Preparation of magnesium oxide confined in activated carbon synthesized from palm kernel shell and its application for hydrogen sulfide removal. *IOP Conference Series: Earth and Environmental Science* **2022**, *963* (1), 012031.
(161) Guo, J. X.; Fan, L.; Peng, J. F.; Chen, J.; Yin, H. Q.; Jiang, W. J. Desulfurization activity of metal oxides blended into walnut shell based activated carbons. *J. Chem. Technol. Biotechnol.* **2014**, *89* (10), 1565−1575.
(162) Sumathi, S.; Bhatia, S.; Lee, K. T.; Mohamed, A. R. Cerium impregnated palm shell activated carbon (Ce/PSAC) sorbent for simultaneous removal of SO2 and NO—Process study. *Chemical Engineering Journal* **2010**, *162* (1), 51−57.
(163) Tian, Y. S.; Zhou, X.; Wang, C. Y.; Zhou, P.; Wang, W. L.; Song, Z. L.; Zhao, X. Q. Desulfurization characteristics and mechanism of iron oxide-modified bio-carbon materials. *Energy* **2022**, *258*, 124865, .
(164) Ma, Q.; Chen, W.; Jin, Z.; Chen, L.; Zhou, Q.; Jiang, X. One-step synthesis of microporous nitrogen-doped biochar for efficient removal of CO_2 and H_2S. *Fuel* **2021**, *289*, 119932, .
(165) Chen, L.; Jiang, X.; Ma, S.; Chen, W.; Xu, B.; Dai, Z.; Jiang, W.; Peng, Y.; Li, J. Towards highly exposed active sites via Edge-N-rich carbon nanosheet @ porous biochar for efficient H_2S catalytic oxidation. *Chemical Engineering Journal* **2023**, *475*, 146115, .
(166) Shao, J.; Zhang, J.; Zhang, X.; Feng, Y.; Zhang, H.; Zhang, S.; Chen, H. Enhance SO2 adsorption performance of biochar modified by CO2 activation and amine impregnation. *Fuel* **2018**, *224*, 138−146.
(167) Ning, P.; Liu, S.; Wang, C.; Li, K.; Sun, X.; Tang, L.; Liu, G. Adsorption-oxidation of hydrogen sulfide on Fe/walnut-shell activated carbon surface modified by NH3-plasma. *Journal of Environmental Sciences* **2018**, *64*, 216−226.
(168) Zhao, Y.; Liu, Y. Study on Removal of Gaseous Hydrogen Sulfide from Straw Biochar Modified by Fenton-Like Waste Solution and Ultraviolet Light. Jiang Su University, 2023.
(169) Chen, G.; Jin, Y.; Lu, J. Experimental study on adsorption of SO2 and DCM from air pollutants by modified biochar. *Biomass Conversion and Biorefinery* **2024**, *14*, 15705.
(170) Sun, X.; Ruan, H.; Song, X.; Sun, L.; Li, K.; Ning, P.; Wang, C. Research into the reaction process and the effect of reaction conditions on the simultaneous removal of H2S, COS and CS2 at low temperature. *RSC Adv.* **2018**, *8* (13), 6996−7004.
(171) Min, L.; Zhihong, Z.; Yan, W. Adsorption of Low Concentration of Carbonyl Sulfide by Cu, Ag Modified Activated Carbon at Ambient Temperature. *Fine Chemicals* **2016**, *33* (04), 390−395.
(172) Perry, W. L.; Datye, A. K.; Prinja, A. K.; Brown, L. F.; Katz, J. D. Microwave heating of endothermic catalytic reactions: Reforming of methanol. *AIChE J.* **2002**, *48* (4), 820−831.
(173) Yang, W.; Li, Y.; Shi, S.; Chen, H.; Shan, Y.; Liu, Y. X. Mercury removal from flue gas by magnetic iron-copper oxide modified porous char derived from biomass materials. *Fuel* **2019**, *256*, 115977, .
(174) Cui, S. B.; Shan, Y.; Liu, Y. X. Hg0 Removal by Straw Biochars Prepared with Clean Microwave/H2O2Modification. *Chem. Eng. Technol.* **2021**, *44* (8), 1460−1469.
(175) Li, Y.; Liu, Y. X.; Yang, W.; Liu, L.; Pan, J. F. Adsorption of elemental mercury in flue gas using biomass porous carbons modified by microwave/hydrogen peroxide. *Fuel* **2021**, *291*, 120152, .
(176) Xu, W.; Hussain, A.; Liu, Y. A review on modification methods of adsorbents for elemental mercury from flue gas. *Chemical Engineering Journal* **2018**, *346*, 692−711.
(177) Zhang, B.; Xu, P.; Qiu, Y.; Yu, Q.; Ma, J.; Wu, H.; Luo, G.; Xu, M.; Yao, H. Increasing oxygen functional groups of activated carbon with non-thermal plasma to enhance mercury removal efficiency for flue gases. *Chemical Engineering Journal* **2015**, *263*, 1−8.
(178) Zhang, J.; Duan, Y.; Zhou, Q.; Zhu, C.; She, M.; Ding, W. Adsorptive removal of gas-phase mercury by oxygen non-thermal plasma modified activated carbon. *Chemical Engineering Journal* **2016**, *294*, 281−289.
(179) Xie, J. Z.; Zhang, C. Y.; Waite, T. D. Hydroxyl radicals in anodic oxidation systems: generation, identification and quantification. *Water Res.* **2022**, *217*, 118425, .
(180) Li, S.; Yang, Y. L.; Zheng, H. S.; Zheng, Y. J.; Jing, T.; Ma, J.; Nan, J.; Leong, Y. K.; Chang, J. S. Advanced oxidation process based on hydroxyl and sulfate radicals to degrade refractory organic pollutants in landfill leachate. *Chemosphere* **2022**, *297*, 134214, .
(181) Liu, Y. X.; Cui, S. B.; Wu, P. J.; Liu, L.; Dou, Z. F.; Wang, Y. Removal of gaseous elemental mercury using corn stalk biochars modified by a green oxidation technology. *Fuel Process. Technol.* **2023**, *242*, 107621.
(182) Wang, Y.; Ma, C.; Dou, Z. F.; Liu, Y. X. Simultaneous removal of SO_2, NO and Hg0 using porous carbon/heat-coactivated persulfate system. *Fuel Process. Technol.* **2023**, *244*, 107698.
(183) Guo, S. P.; Wang, Q.; Luo, C. J.; Yao, J. G.; Qiu, Z. P.; Li, Q. B. Hydroxyl radical-based and sulfate radical-based photocatalytic advanced oxidation processes for treatment of refractory organic matter in semi-aerobic aged refuse biofilter effluent arising from treating landfill leachate. *Chemosphere* **2020**, *243*, 125390, .
(184) Yang, Y.; Shi, Y. X.; Cai, N. S. Simultaneous removal of COS and H2S from hot syngas by rare earth metal-doped SnO2 sorbents. *Fuel* **2016**, *181*, 1020−1026.
(185) Wang, Y.; Wu, X.; Wei, D.; Chen, Y.; Yang, J.; Wu, L. Research progress on adsorption and separation of carbonyl sulfide in blast furnace gas. *RSC Adv.* **2023**, *13* (18), 12618−12633.
(186) Gao, S.; Zhao, S.; Tang, X.; Wang, Y.; Yi, H. Mechanics of COS removal by adsorption and catalytic hydrolysis: Recent developments. *Fuel* **2024**, *359*, 130394, .
(187) Sattler, M. L.; Rosenberk, R. S. Removal of Carbonyl Sulfide Using Activated Carbon Adsorption. *J. Air Waste Manage. Assoc.* **2006**, *56* (2), 219−224.
(188) Hanaoka, T.; Hiasa, S.; Edashige, Y. Syngas production by gasification of aquatic biomass with CO2/O2 and simultaneous removal of H2S and COS using char obtained in the gasification. *Biomass and Bioenergy* **2013**, *59*, 448−457.

https://doi.org/10.1021/acs.energyfuels.4c06274
Energy Fuels XXXX, XXX, XXX−XXX

(189) Li, P. F.; Wang, G. C.; Dong, Y.; Zhuo, Y. Q.; Fan, Y. M. A Review on Desulfurization Technologies of Blast Furnace Gases. *Current Pollution Reports* **2022**, *8* (2), 189−200.
(190) Kim, J.; Do, J. Y.; Nahm, K.; Park, N.-K.; Chi, J.; Hong, J.-P.; Kang, M. Capturing ability for COS gas by a strong bridge bonding of a pair of potassium anchored on carbonate of activated carbon at low temperatures. *Sep. Purif. Technol.* **2019**, *211*, 421−429.
(191) Wang, Y.; Ding, L.; Long, H.; Xiao, J.; Qian, L.; Wang, H.; Xu, C. Carbonyl sulfur removal from blast furnace gas: Recent progress, application status and future development. *Chemosphere* **2022**, *307*, 136090, .

https://doi.org/10.1021/acs.energyfuels.4c06274
Energy Fuels XXXX, XXX, XXX−XXX